THE UNIVERSITY OF MICHIGAN

COLLEGE OF ENGINEERING
Department of Mechanical Engineering
Heat Transfer and Thermodynamics Laboratory

Progress Report No. 3

(For the Period August—November, 1961)

# PRESSURIZATION OF LIQUID OXYGEN CONTAINERS

J. A Clark
H. Merte, Jr.
V. S. Arpaci
P. S. Larsen
P. Fennema
J. Beukema
H. Law
H. C. Totten
B. Bailey
W. J. Yang

ORA Project 04268

under contract with:

NATIONAL AERONAUTICS AND SPACE ADMINISTRATION
GEORGE C. MARSHALL SPACE FLIGHT CENTER
CONTRACT NO. NAS-8-825
HUNTSVILLE, ALABAMA

administered through:

OFFICE OF RESEARCH ADMINISTRATION ANN ARBOR

March 1962

TABLE OF CONTENTS


| | Page |
|---|---|
| LIST OF FIGURES | v |
| NOMENCLATURE | vii |
| ABSTRACT | xi |
| I. OPTIMIZATION OF PRESSURIZED DISCHARGE PROCESSES IN CRYOGENIC CONTAINERS | 1 |
| A. Experimental Program | 1 |
| B. Analytical Program | 2 |
| II. BOILING OF A CRYOGENIC FLUID UNDER REDUCED GRAVITY | 7 |
| A. Additional Data | 7 |
| 1. 1-Inch-Diameter Copper Sphere | 7 |
| a. $a/g = 1$ | 8 |
| b. $a/g \approx 0$ | 8 |
| 2. 1/2-Inch-Diameter Copper Sphere | 8 |
| a. Film boiling, $a/g = 1$ | 9 |
| b. Transition and nucleate boiling, $a/g = 1$ | 9 |
| B. Future Work | 10 |
| III. HEAT TRANSFER TO A CRYOGENIC FLUID IN AN ACCELERATING SYSTEM | 11 |
| IV. INJECTION COOLING | 13 |
| A. Lumped System | 13 |
| 1. Analysis | 13 |
| a. Introduction | 13 |
| b. Gas injection with liquid phase present only | 16 |
| c. Gas injection with two-phase equilibrium | 18 |
| d. Solutions | 21 |
| e. Discussion of solutions. Effect of gas solubility | 25 |
| 2. LOX-Systems Cooled by He-Injection | 26 |
| 3. $LH_2$-Systems Cooled by He-Injection | 27 |

TABLE OF CONTENTS (Concluded)


| | Page |
|---|---|
| B. Bubble Dynamics of a Distributed System | 28 |
| 1. Heat and Mass Diffusion in a Moving Medium with Time-Dependent Boundaries | 28 |
| 2. Application of the Theory in IV-B-1 to Bubble Growth | 29 |
| a. Bubble growth in a boiling liquid | 29 |
| b. Bubble growth in a binary system | 31 |
| c. Bubble growth of noncondensing gas in cryogenic liquids | 33 |
| APPENDIX I | 37 |
| APPENDIX II | 39 |
| REFERENCES | 43 |

LIST OF FIGURES

Figure


1. Inlet Piping Assembly.

2. Analog Computer Circuit for a Typical Node.

3. Boiling Heat Transfer to Liquid Nitrogen at Atmospheric Pressure from 1-in.-Diameter Copper Sphere at a/g = 1 and 0.

4. Nucleate-Boiling Heat-Transfer Data of Liquid Hydrogen at a/g = 1 and a/g = 0.

5. Boiling Heat-Transfer Data of Liquid Nitrogen at a/g = 1 Showing Influence of $O_2$ Impurity.

6. Film-Boiling Heat-Transfer Data of Liquid Nitrogen at a/g $\approx$ 0.

7. Film-Boiling Heat-Transfer Data of Liquid Nitrogen at a/g = 1 and a/g $\approx$ 0.

8. Boiling Heat-Transfer Data of Liquid Nitrogen at a/g = 1 and a/g $\approx$ 0.

9. Boiling Heat-Transfer Data of Liquid Nitrogen at a/g = 1 and a/g $\approx$ 0.

10. Boiling Heat-Transfer Data of Liquid Nitrogen at a/g = 1 and a/g $\approx$ 0.

11. Analytical Model for Gas Injection with Liquid Phase Present Only.

12. Tentative Hydrogen-Helium Equilibrium.

13. Analytical Model for Gas Injection with Two-Phase Equilibrium.

14. Space-Time Domain for Heat-Conduction Problem with a Moving Boundary.

NOMENCLATURE

| | |
|---|---|
| $A$ | property group $[1/(T_A-T_B)](h_{fgA}v'_A/c'_A v'')(\dot{V}_B/V_S)$ |
| $A_1$ | property group $A/[1-G(1+1/X_\infty)]$ |
| $B$ | property group $[1/(T_A-T_B)](dT/dt)_o$ |
| $C$ | property group $\Delta h_B/h_{fgA}$ |
| $C_1$ | constant |
| $c$ | Molal specific heat |
| $D$ | property group, $D = B/A + C$ |
| $D_1$ | property group, $D_1 = B/A_1 + C$ |
| $\mathcal{D}$ | mass diffusivity |
| $E$ | property group $[1/(T_A-T_B)](h_{fgA}/c'_A)$ |
| $F$ | property group $h_{fgB}/h_{fgA}$ |
| $G$ | property group $(\ell/U)(\dot{V}_B/V_S)$ |
| $G(\bar{r},\bar{r}',t)$ | Green's function for Eq. (45) |
| $h$ | enthalpy per mole |
| $h_{fg}$ | heat of evaporation per mole |
| $\Delta h_B$ | enthalpy change per mole of injected gas when cooled from its initial temperature to system temperature |
| $K$ | property group $c'_B/c'_A$ |
| $L$ | property group $v'_B/v'_A$ |
| $\ell$ | length of system |
| $N$ | property group $(v'_A/v'')(\dot{V}_B/V_S)$ |
| $n$ | moles |

| | |
|---|---|
| $P$ | pressure |
| $q$ | rate of heat transfer |
| $Q_T$ | strength of instantaneous point sink of heat |
| $Q_M$ | strength of instantaneous point source of mass |
| $Q_C$ | strength of instantaneous point sink of mass |
| $\bar{r}$ | radius vector in the fluid |
| $\bar{r}_o$ | radius vector of the moving boundary |
| $R$ | radius of bubble |
| $T$ | temperature |
| $T(\bar{r},t)$ | temperature of the fluid |
| $T_1(\bar{r},t)$ | temperature of the fluid for the case of the moving boundary takes the path from A to C to B (Fig. 14) |
| $T_2(\bar{r},t)$ | temperature of the fluid for the case of the moving boundary takes the path from A to D to B (Fig. 14) |
| $t$ | time |
| $u(\bar{r},t)$ | local fluid velocity |
| $U$ | average velocity of rising gas bubbles |
| $v$ | Molal specific volume |
| $V$ | volume |
| $\dot{V}_B$ | volume-rate of helium at system temperature and pressure |
| $x_A$ | mole fraction of component A in gas phase |
| $x_B$ | mole fraction of component B in gas phase |
| $X$ | ratio of mole fractions in gas phase, $(1-x_A)/x_A$ |
| $y$ | time variable, between $t = 0$ and $t = t$ |

| | |
|---|---|
| $z_A$ | mole fraction of component A in liquid phase |
| $z_B$ | mole fraction of component B in liquid phase |
| $Z$ | ratio of mole fractions in liquid phase $(1-z_A)/z_A$ |
| $\alpha$ | thermal diffusivity of liquid |
| $\gamma_n$ | eigen-value, defined by Eq. (64) |
| $\delta_A$ | property group $(h_{fgA}v'_A/c'_Av'')$ |
| $\epsilon$ | slope of non-dimensional boiling curve $(T_A-T_B)/(T_A-T_Z)$ |
| $\theta$ | non-dimensional temperature $(T-T_B)/(T_A-T_B)$ |
| $\Theta$ | temperature of the fluid at C' or B' in Fig. 14 |
| $\theta_Z$ | non-dimensional temperature $(T_Z-T_B)/(T_A-T_B)$ |
| $\lambda$ | coefficient of bubble growth, dimensionless |
| $\xi$ | time variable ranging from t = y to t = t |
| $\rho$ | Molal specific density |

SUBSCRIPTS

| | |
|---|---|
| A | Component A. Saturation state, where used with T or p |
| B | Component B. Saturation state, when used with T or p |
| G | gas |
| i | inlet condition |
| L | liquid |
| sub | subcooling |
| S | total for system |
| s | at bubble interface |

| | |
|---|---|
| o | initial value |
| ∞ | asymptotic value; at a distance from the bubble interface |

SUPERSCRIPTS

| | |
|---|---|
| " | gas phase |
| ' | liquid phase |

Time derivations are indicated by a "dot" ($\cdot$)

ABSTRACT

I. Optimization of Pressurized Discharge Processes in Cryogenic Containers

Modifications to the experimental apparatus for high inlet gas temperatures are described. A new method for analysis of the pressurized discharge process is discussed. This involves the use of an analog computer, through which axial diffusion and convective effects can be studied.

II. Boiling of a Cryogenic Fluid Under Reduced Gravity

Additional experimental data for boiling of liquid nitrogen from a 1-in.-diameter sphere in the film-boiling region under free-fall conditions are presented. The effect of liquid nitrogen contaminated with oxygen is shown for $a/g = 1$.

Experimental data for boiling of liquid nitrogen from a 1/2-in.-diameter sphere are presented over the entire boiling range with free fall, indicating little size effect.

In the nucleate boiling region, reduction of the buoyant forces with free fall appears to have negligible effect on the heat-flux—temperature difference relationship.

III. Heat Transfer to a Cryogenic Fluid in an Accelerating System

Preparation of the experimental apparatus is continuing. Construction of the redesigned flat-plate heater was completed during this period. During a preliminary test of the system with liquid nitrogen, the skirt guard heater burned out. This unit is being repaired.

## IV. Injection Cooling

The general lumped system transient is formulated for the cooling of a cryogenic liquid in a vertical column by gas injection at the bottom, and represents the limiting case of the injection of infinitesimal small bubbles. The effects of gas solubility in the liquid phase, gas enthalpy flux, and ambient heating are included. The presence of rising gas bubbles has been considered in evaluating the system's heat capacity.

The analysis is expected to apply to $He-O_2$ systems under the assumption of zero liquid solubility of the gas, while finite solubility must be considered for $He-H_2$ systems.

The solution for the asymptotic temperature, approached by continued injection, and approximate solutions for the temperature transient, valid for zero and low liquid solubilities of the gas, are presented.

The asymptotic temperature is essentially unaffected by the liquid solubility of the gas. Finite gas solubility, however, decreases the rate of cooling.

An approximate method is reviewed for solving the problem of heat diffusion in a moving medium with time-dependent boundaries. The method is applied to the problem of a growing bubble in, respectively, a one- and two-component boiling liquid, in the latter case considering the simultaneous mass and heat transport in the liquid.

Comparison with exact solutions of the problem of bubble growth in boiling liquids confirms the usefulness of the approximate method in this case.

Next, the method is applied to predict growth rates of helium bubbles in liquid oxygen and nitrogen.

# I. OPTIMIZATION OF PRESSURIZED DISCHARGE PROCESSES IN CRYOGENIC CONTAINERS

## A. Experimental Program

As discussed in Ref. 1, a problem was encountered in eliminating the inlet-gas-temperature transient caused by the piping immediately preceding the container. An attempt has been made to correct this condition by utilizing the bleed-off gas as a means of heating the piping. This proved to be ineffective. During the past period, electrically insulated heating wire was wound around the piping using a thermal conducting cement (Thermon T63) which has a relatively high thermal conductivity. The cement serves to bond the heating wire to the inlet piping and to even out the heat flux applied to the piping. Nine thermocouples were installed at significant locations on the heating wire and piping, and these were connected to a millivolt meter to enable matching the temperature of the piping with that of the inlet gas. Due to the configuration of the piping and the desirability of being able to disassemble the piping, it was necessary to wire the heaters in seven separate elements. The original intent was to connect all seven elements in a series-parallel combination to permit control by means of a single Variac. However, after testing numerous combinations, it was found to be virtually impossible to get the same temperature throughout the length of the piping using the one Variac. Since three other Variacs were available in the laboratory, four Variacs are now used to control the temperature of the inlet piping. This has proved to be very satisfactory on subsequent runs in providing a rapid temperature response and accurate control.

The inlet-gas-temperature measurement prior to this time has been obtained using a single 24-ga. thermocouple. This single thermocouple has been replaced by four 30-ga. thermocouples as shown in Fig. 1. It may be seen that the thermocouple numbered 1 is in essentially the same position as the previously used single 24-ga. thermocouple. The thermocouples are suspended from above by a gland-type fitting which has lava as a sealant. The purpose of using four thermocouples is to provide a means of checking one thermocouple reading against the others, for the measurement of the important parameter $T_g$. A switching device is incorporated into the thermocouple circuit to the Sanborn recording unit so that each thermocouple may be recorded individually.

A set of experimental runs, numbered 57 A through O, were obtained and reduced during this period. It was expected that the four inlet-gas thermocouples would indicate essentially the same temperature level, but this proved not to be the case. Inlet thermocouples 2, 3, and 4 indicated almost the same temperature, but their difference was erratic; sometimes No. 2 read highest and sometimes No. 3. Investigation showed this to be a direct result of using only one Variac, as described above, to control the power into each heating

element on the inlet piping, and was subsequently corrected by the use of four Variacs. The largest discrepancy was noted between inlet thermocouples 1 and 2, with 1 reading consistently lower, as much as 200° at a level of 500°F, than thermocouple 2. On a plot of mean density versus inlet temperature, neither temperature correlated very well with the theoretical curve. Difficulty also was experienced with the liquid-level indicator during these runs. The float would rise with the liquid level to about two-thirds of the height of the tank, and would then get caught and remain in a fixed position. In an attempt to correct this, the bottom of the container was removed. It was then discovered that the Foamglas insulation in the top of the main container had broken away from its supports and was lying on top of the baffle plate, blocking the flow of gas through the desired opening. The pressurant was flowing between the top of the Foamglas insulation and the aluminum container top instead of directly into the ullage space. This evidently caused the large difference in temperature between the inlet thermocouples 1 and 2. On the basis of this, runs numbered 57 are considered unreliable and will not be reported.

To correct this problem, since Foamglas does not have much rigidity in itself, a copper framework with a skin of 0.005-in. brass shim stock soldered to it was devised to enclose the insulation. The whole assembly was also secured to the top of the container with one additional screw. Since the brass shim stock is very thin and only the edges of the copper strips which comprise the framework are exposed to the gas space, the characteristics of the system with regard to heat-transfer interaction with the top of the container have not been significantly changed.

The difficulty encountered with the liquid-level indicator sticking, as mentioned above, has been corrected. It was found that the sections of ceramic tubing which enclose the thermocouple leads to the floating thermocouples were catching between two screws which protruded from the framework in the bottom of the container. After these protruding ends were cut off, the float was able to rise freely with the liquid interface.

With the above modifications and corrections completed, the system appears to be ready for operation. It is expected that in the very near future, high-inlet-temperature data will be taken and reported.

## B. Analytical Program

In previous studies[1] the dynamic response of the process of pressurized discharge of a cryogenic liquid from a container was investigated for simultaneous, multiple, time-dependent disturbances of an arbitrary form in the inlet-fluid temperature, the ambient temperature, and/or the ambient heat flux. In the formulation of the problem, the axial conduction both in the wall and pressurant were neglected. Hence the solutions were obtained in terms of

inlet pressurant gas temperature only. However, when the interface temperature difference between the pressurant and liquid increases, or when the area of this interface becomes an important fraction of the total surface wetted by the pressurant, the effect of the liquid temperature becomes equally important, and must be included in the formulation of the problem. This effect is suggested by the sketch.

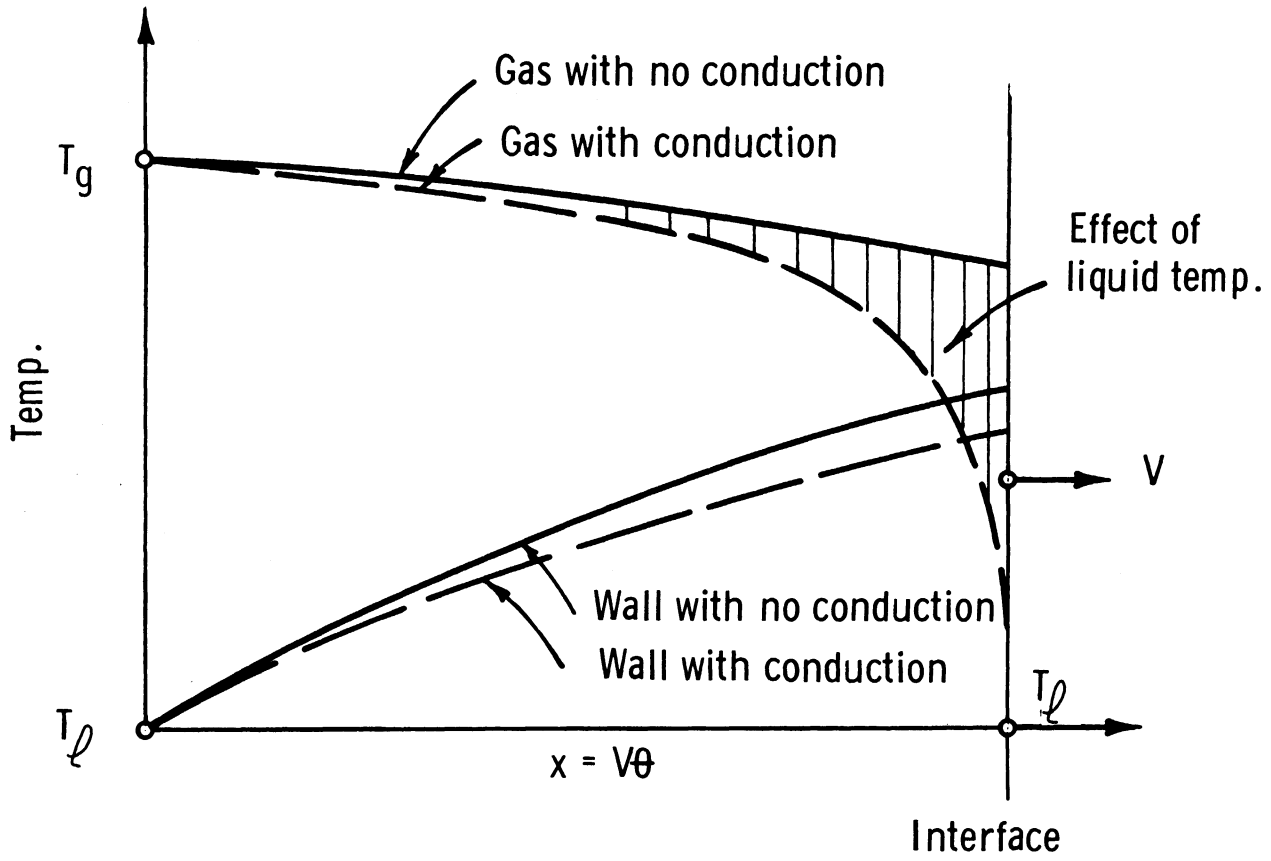


The axial molecular conduction is greater in the wall than the pressurant, for most tank geometries, but the pressurant conductivity in the present analysis includes the eddy conductivity as well as molecular conductivity. However, since the primary concern of the present study is to include the effect of liquid pressurant interface temperature on the temperature distribution in the pressurant regardless of the relative importance of the pressurant and wall conductivities, the axial conduction in the wall is neglected. It is expected that such an effect can and will be considered in subsequent analysis, but will require a more complex analog computer circuit.

An insulated container is considered as a first model for study in the new analysis. The transient phenomenon is introduced by the temperature difference between the pressurant and the liquid and wall.

The application of the first law to a radially lumped fluid control volume and a wall system produces the two differential equations following, one for

the pressurant gas and one for the wall:

$$\frac{\partial T}{\partial \theta} + V\frac{\partial T}{\partial x} + \frac{\bar{h}_g P}{PC_p A}(T - t) + (\alpha + \epsilon_h)\frac{\partial^2 T}{\partial x^2} = 0 \qquad (1)$$

$$\frac{\partial t}{\partial \theta} - \frac{\bar{h}_g P}{\rho' C_p' A'}(T - t) = 0 \qquad (2)$$

with the initial and boundary conditions

$$T(x,0) = 0, \qquad (3)$$

$$t(x,0) = 0, \qquad (4)$$

$$T(0,\theta) = T_g(\theta) - T_e, \qquad (5)$$

$$T(V\theta,\theta) = 0, \qquad (6)$$

where the temperatures (above the saturation temperature of the liquid), density, specific heat, and cross-sectional area of the gas and wall are $T(x,\theta)$, $t(x,\theta)$, $(\rho,\rho')$, $(C_p,C_p')$ and $(A,A')$, respectively. The heat-transfer coefficient is $\bar{h}_g$, the interface periphery P, the axial distance x, the time $\theta$, molecular and eddy diffusivities of the fluid are $\alpha$ and $\epsilon_h$. An attempt has been made to solve the foregoing simultaneous, partial differential equations by a method similar to previous analytical studies. The resulting Laplace transforms are not readily available in tables, and furthermore, the use of inversion theorem yields a rather involved contour integration. More specifically, the mathematical difficulty comes from the inverse transformation of

$$e^{\pm[1 + P(P + \alpha)/\beta(P + \gamma)]^{1/2}} \qquad (7)$$

combined with other but simpler transform functions. Because of the practical problems associated with this, another approach is planned in solving the equations, at least for the initial phase of the study. From the standpoint of the University's facilities, a numerical or analogical procedure can well be used. However, consistent with the approximation involved in the heat-transfer coefficient $\bar{h}_g$, assumptions of incompressibility, etc., a less accurate but faster and more convenient method of solution can be obtained using the analog computer.

The height of the container is divided into ten equal parts. Then, for a typical nodal point, the explicit form of the analog circuit is given in Fig. 2

which leads to the following finite difference equations:

$$\frac{dT_n}{d\theta} + \left(\frac{T_{n+1} - T_{n-1}}{R_o C}\right) + \left(\frac{T_n - t_n}{R_1 C}\right) - \left(\frac{T_{n+1} + T_{n-1} - 2T_n}{RC}\right) = 0, \qquad (8)$$

$$\frac{dt_n}{d\theta} - \left(\frac{T_{n+1} - T_{n-1}}{R_2 C}\right) = 0, \qquad (9)$$

where the variable resistances $R_o$ and R are related to the length $\Delta x$ which varies during the discharge process. Actually, the variation of $\Delta x$ will be introduced by the proper use of multiplier and function generator units of the available analog computer, which is a Pace Model 16-31R-4.

One of the most important features of the new analysis is that it includes the axial eddy diffusivity $\epsilon_h$ of gases. Hence, along the interface, the axial and turbulent heat-transfer coefficient between the pressurant and liquid can readily be calculated from the resulting solutions by their comparison with experimental data of temperature profiles in the region of the pressurant gas-liquid interface.

## II. BOILING OF A CRYOGENIC FLUID UNDER REDUCED GRAVITY

Figure 3 is a reproduction of data reported in Ref. 1, which provides a graphic comparison with current boiling heat-transfer correlations as well as with the experimental work of others. In the nucleate boiling region, reduction of the buoyant forces with free fall appears to have negligible effect on the heat flux-temperature difference relationship.

Similar effects have been observed for nucleate boiling of liquid hydrogen, using both aircraft and 1-second laboratory free-fall tests to obtain zero gravity. Figure 4, reproduced from Ref. 7, shows the results obtained using liquid hydrogen. A flat heating surface was used, with the energy source provided by resistance heating of a thin lead film deposited on a glass insulating substrate. The temperature of the heating surface was determined by measuring the change in resistance of the metallic film. No detailed information is available, but it is possible that the heat capacity of the substrate would influence the results.

### A. Additional Data

During the early part of the past reporting period some additional free-fall data were obtained with the spheres. Subsequently, a premature drop caused extensive damage to the test platform. The damage was a consequence of the test object being external to the test vessel at the time of premature release and inducing turning moments on the platform as it dropped. The guide-wire end hooks opened and the test platform did not land on the buffer piston.

The test platform has been repaired and the release mechanism has been redesigned so that premature release of the test platform cannot take place. Opportunity was taken at this time to begin rewiring the entire electrical system to make it ready for operation at reduced gravities other than zero. This will require about 3 months, and a description of the new system will be included in the next report.

#### 1. 1-INCH-DIAMETER COPPER SPHERE

As a result of the damage sustained by the premature drop a new 1-in.-diameter copper test sphere was constructed with 2 differential thermocouples at 2 surface locations to permit simultaneous measurements of 2 surface-center temperature differentials. At the peak heat flux the differential was

observed to be approximately the same as for the previous sphere, a maximum of 2°F.

a. $a/g = 1$.—In Ref. 1 data were presented for tests in which the liquid nitrogen was of unknown purity. To substantiate the validity of these data, a number of new tests were conducted at $a/g = 1$ in both the film- and nucleate-boiling regions in which liquid nitrogen having a wide range of $O_2$ impurity was used. Figure 5 shows the results of these tests. Runs after Test No. 21 were conducted using the 1-in. copper sphere having 2 differential thermocouples installed. A gas analyzer is now present at the test facility so that all the liquid nitrogen used is tested for purity.

In the film-boiling range in Fig. 5 increasing nitrogen purity results in a slight downward shift. The dashed line represents results of previous tests for which nitrogen purity measurements were not made.

In the transition and nucleate-boiling regions, a distinct shift to the left is noted in the temperature differences as the nitrogen purity is increased, although the value of the peak heat flux does not appear to be significantly changed. In all cases the fluid temperature was taken as the saturation temperature of pure liquid nitrogen. With 33 mole % of oxygen, the equilibrium saturation temperature is only about 4°F displaced from that of pure nitrogen, but with rapid boiling the condition is far from equilibrium and very likely the liquid near the boiling interface is highly enriched in oxygen. If a saturation temperature nearer to that of pure oxygen were used, the data points for the highly impure nitrogen would be placed in closer agreement with the remaining data.

In Test No. 29-B with purer liquid nitrogen, a discrepancy exists in the transition region. In the particular test the sensitivity of the recorder was decreased by 1/2, and it is possibly an inherent inaccuracy due to the difficulty of measuring slopes of temperature-time in this region.

b. $a/g \approx 0$.—Additional data in the film boiling region were obtained under free-fall conditions with the 1-in.-diameter sphere, and are presented in Fig. 6. With some scatter in the previously reported data, these results provide additional confirmation of the effect of free fall on film boiling.

## 2. 1/2-INCH-DIAMETER COPPER SPHERE

A smaller copper sphere, 1/2-inch in diameter, was constructed to determine what effect size might have on the results. Any errors introduced due to treating the larger sphere as a lumped system should be reduced since decreasing the diameter decreases the maximum Biot Number by a corresponding amount. Because of the smaller size, only one thermocouple could conveniently be inserted, and this was placed at the center. As with the larger sphere, a 1/32-in.-diameter hole was drilled and the thermocouple junction was soldered at the bottom of the hole.

a. Film Boiling, a/g = 1.—Figure 7 shows data obtained for film boiling both at a/g = 1 and free fall. Also included for reference are the curves representing data obtained with the 1-in.-diameter sphere. Excellent agreement exists between the data for the two different sizes at a/g = 1.

With free fall the trend with the small sphere is similar to that for the larger one. That is, the heat flux was of a finite magnitude and decreased with a decrease in $\Delta t$. It is noted that the heat flux at the higher $\Delta t$ is larger than for the 1-in. sphere and lower near the transition region. The slope of heat flux versus $\Delta t$ with free fall is quite parallel to that at a/g = 1. This does suggest a geometrical effect, and may be related to the hydrodynamic behavior of the liquid with film boiling under near-zero body forces. In all cases the sphere was precooled before insertion into the liquid nitrogen. It is believed that any residual liquid motion during free fall did not materially affect the results.

b. Transition and Nucleate Boiling, a/g = 1.—Figure 8 shows data obtained for a/g = 1 through the transition, peak, and nucleate-boiling regions. One free-fall test is included where release took place in the nucleate-boiling region.

The behavior at a/g = 1 is similar to that with the 1-in. sphere except in the transition zone, where the temperature difference is shifted to lower values. This change may be a size effect, or may represent the error due to treating the larger sphere as a lumped system. With the larger sphere both the surface and center temperature transients were used to calculate the heat flux, and the differences were small, indicating that size may be the dominant factor. As will be described, a computer program is being written to examine further the error due to treating the sphere as a lumped system.

The maximum heat flux with the 1/2-in.-diameter sphere is the same as that obtained with the 1-in. sphere, and behavior in the nucleate region with free fall is also the same as was previously observed.

Figure 9 shows the results of 2 test runs in which the test package was released at two separate points in the transition region. For Test No. 28B the heat flux had begun to rise when release took place, decreased upon release, and then again rose during free fall.

For Test No. 28F the data before release compare quite well with those of Fig. 8. Upon release the heat flux decreased, then increased to approximately the same maximum value obtained with the 1-in. sphere under free fall conditions, and followed the same nucleate-boiling behavior as before. As a consequence of the small size, it is possible to cover a greater portion of the transition—nucleate-boiling region in the 1.4-second free-fall time available than was possible with the 1-in. diameter sphere. The similarity of the results may aid in evaluating the validity of extrapolating the short free-fall behavior in transition and nucleate boiling to longer free-fall periods.

Figure 10 presents the results of tests similar to those of Fig. 9, but immediately after release the heat flux experienced a pronounced decrease before increasing further. In the case of Test No. 28E an oscillation in heat flux is evident, indicating perhaps an instability in the boiling process in this region. The transition region has been characterized as an unstable phenomena by Zuber[8] and others for 1-g force fields.

## B. Future Work

Precooling the spheres while investigating film boiling with free fall appeared to have no effect upon the results obtained. To investigate further the question of residual liquid motion, it is planned to conduct several tests in which the liquid nitrogen is to be artificially set in motion during free fall by means of a propeller. This system will produce effects similar to those expected in forced convection.

With the spherical test objects used, a lumped system was assumed in the reduction of the data. To serve as a check on the validity of this assumption in the transition and nucleate-boiling range, a numerical solution of the transient conduction process in a sphere, using a finite-difference technique, is being programmed for the IBM-709 digital computer using as input data the experimental time-temperature measurements near the surface of the sphere. The heat flux determined can then be compared with that obtained by the present technique, and the computed center-surface temperature differentials can be compared with experimental measurements.

It is anticipated that, once the program has been written and proven, it will greatly facilitate the reliable reduction of data, at present a time-consuming process.

The problems involved in studying the boiling of liquid hydrogen with the present free-fall facility are being considered. It is believed that the transient technique employed will be entirely suitable for liquid hydrogen. This will be aided by the low peak heat flux of approximately 24,000 Btu/hr-ft$^2$ as presented in Ref. 7. Reliable $C_p$ data for copper at liquid hydrogen temperatures will be required.

# III. HEAT TRANSFER TO A CRYOGENIC FLUID IN AN ACCELERATING SYSTEM

Construction of the redesigned flat-plate heater as described in Ref. 1 was completed during this period. During a preliminary test of the system with liquid nitrogen, the skirt guard heater burned out. To determine the cause of the burnout and for repair, the entire system must be disassembled. This will be accomplished during the next reporting period.

# IV. INJECTION COOLING

## A. Lumped System

### 1. ANALYSIS

a. Introduction.—In a previous study[1] a lumped system analysis of injection cooling was made under the limiting condition of zero liquid solubility of the injected gas, which furthermore was assumed injected at system temperature. In addition, no correction was made for the decrease in heat capacity of the system due to the presence of rising gas bubbles causing a decrease in liquid volume. In the present study the lumped analysis is extended to obviate these limiting assumptions.

The process of injection cooling is intimately associated with the phase-equilibrium characteristics of the binary system composed of component A (liquid to be cooled) and component B (injected gas). The effectiveness of injection cooling is primarily a question of creating and maintaining in the liquid cavities or bubbles, initially having a zero vapor pressure of component A, such that evaporation of A can proceed until thermodynamic phase equilibrium is established between the vapor mixture in the cavity and the surrounding liquid. Therefore low solubility of the injected gas in the liquid phase is of significance. Phase equilibria for substances with highly deviating critical states usually result in low liquid solubility of the component with the lower critical state, in particular at states above this. The choice of gases applicable for injection cooling of cryogenic systems is therefore limited to helium, hydrogen, deuterium and neon, of which only the former two seem practical.* For oxygen and nitrogen systems, helium and hydrogen may be used, while only helium is applicable for hydrogen systems. While helium can be considered insoluble in oxygen and nitrogen at moderate cryogenic temperatures, finite gas solubility must be considered for any of the other combinations. Within the limitations of the lumped analysis, the effect of finite gas solubility will therefore be studied in the present analysis.

The subsequent thermal and thermodynamic analysis is based on an isobaric process assuming complete and instantaneous mixing and instantaneous phase equilibrium, achieved at the rate at which the gas is injected into the liquid. By these assumptions the problem is reduced from a space-time-dependent transient to a simple transient of a lumped system, the transient being governed by the injection rate.

---

*Xenon and the other heavier rare gases are excluded a priori since these are not superheated vapors at the cryogenic states considered.

The lumped analysis is justified when the rate at which mass and heat is exchanged between the gas and liquid phases is high compared to injection rates and bubble rise velocities. Further, this analysis assumes a thorough mixing to take place within each phase to eliminate temperature and concentration gradients. The rate of the mass- and heat-transfer process is proportional to the surface area of contact between the two phases, and thus inversely proportional to the bubble size for a given injected gas volume. The lumped analysis consequently gives the solution for the limiting case of zero initial size of the injected gas bubbles.

When a nonsoluble gas is injected into a volatile liquid, the evaporation from the bubble interface resulting in bubble growths and heat removal from the liquid is a process similar to that of bubble-growth in a boiling, super-heated, one-component liquid. The only difference is that growth terminates in the former case when the equilibrium gas composition is reached corresponding to the bulk temperature. In the latter case the bubble growth is continuous under the assumption of constant bulk temperature until thermodynamic equilibrium is obtained consisting of bubbles having infinite radii of curvature and a zero temperature difference between liquid and vapor. The asymptotic stage of growth, representing the main part of the bubble life, is a process limited by the rate of heat transfer from the bulk of the liquid to the interface facilitating the evaporation. Analytical solutions[9] verified by experiments[10] indicate bubble-growth according to

$$\frac{dR}{dt} = \dot{R} = \lambda \sqrt{\frac{\alpha}{t}},$$

where the nondimensional growth constant $\lambda \cong \frac{c'v'}{h_{fg}v''} (T_\infty - T_s)$ is proportional to the superheat, $T_\infty - T_s$, $\alpha$ is the thermal diffusivity of the liquid, and t is the time.

When a partially soluble gas is injected into a volatile liquid, the mass transfer is no longer limited by the heat-transfer process in the liquid alone, but also by the associated mass diffusion processes. The following simultaneous processes will take place when a gas bubble of component B is introduced into a liquid mixture of A and B. At the bubble interface gaseous B will go into liquid solution giving up the latent heat and heat of solution, diffusing into the surrounding liquid. By counter diffusion in the liquid, component A will reach the interface and evaporate into the bubble removing the heat of evaporation from the liquid. In the gas phase, counter diffusion of A and B will take place, and assuming phase equilibrium at the interface, the gas and liquid compositions here are related to the interface temperature. This condition in connection with an interfacial heat and mass balance, ignoring the heat capacity of the gas phase, couples the heat-conduction and convection problem in the liquid phase to the two-region mass-diffusion and convection problem. In a first evaluation of the limiting process, it can be remarked that, since in the liquid the thermal diffusivity is considerably greater than the mass dif-

fusivity, the evaporation rate at the interface cannot be limited by the heat-transfer rate. Further, the mass diffusivity in the gas phase is much greater than that in the liquid, so that the main resistance to mass transfer lies in the liquid film next to the interface. It therefore seems appropriate to expect that the mass diffusion in the liquid will be the limiting process.

A diffusion limited process is exemplified in the common process of absorption of a partially soluble gas injected into a nonvolatile liquid. The analytical solution[11] based on the "penetration theory" and verified experimentally indicates average volume transfer rates, or for bubbles, growth-rates according to

$$\dot{R} = \lambda_M \sqrt{\frac{\mathcal{D}'}{t_{exp}}}$$

where the nondimensional growth-constant, $\lambda_M \cong x_{Bo} - x_{B\infty}$, is proportional to the difference in concentration of the gas at the interface (max. solubility) and in the bulk of the liquid. $\mathcal{D}'$ is the mass diffusivity in the liquid and $t_{exp}$ the exposure time, and $t_{exp} \cong 2R/U$, the bubble diameter divided by the terminal bubble velocity. The analysis assumes an isothermal process and low liquid solubility. As the bubble rises through the liquid, the gas inside the bubble circulates in a toroidal motion, so that it encounters fresh liquid at the top of the bubble, whereby no permanent liquid film adheres to the bubble. If surface active agents contaminate the interface, a considerable decrease in transfer rates is observed.

From the above qualitative discussion it may be expected that in the first approximation, mass-transfer rates for a soluble gas is a factor $(\lambda_M/\lambda)\cdot(\mathcal{D}'/\alpha)^{1/2}$ times those experienced for a nonsoluble gas. Since helium has a finite solubility in liquid hydrogen, the mass-transfer process in this case may be limited by mass diffusion in the liquid. Evaluation of the above factor for this system at an arbitrary temperature of 30°K gives

$$\frac{\lambda_M}{\lambda}\sqrt{\frac{\mathcal{D}'}{\alpha}} \cong \frac{x_{Bo} - x_{B\infty}}{T_\infty - T_S}\frac{h_{fg}v'}{c'v''}\sqrt{\frac{\mathcal{D}'}{\alpha}} \cong \frac{0.02}{5} \cdot 3 \cdot \sqrt{\frac{10^{-5}}{10^{-3}}} = 1.2 \cdot 10^{-3}$$

It has here been assumed that the maximum solubility of helium in hydrogen is 2% by mole fraction, and the superheat for the comparative heat-transfer-governed process has arbitrarily been taken to 5°C. This evaluation shows that if mass diffusion is the limiting process, mass-transfer rates are considerably smaller than if heat transfer were the limiting process, and the lumped analysis may no longer be valid.

The lumped system analysis indicates results in good agreement with experimental data for very low (zero) liquid solubilities of the injected gas.[1] Where

the solubility is considerable, however, the result of the lumped analysis apply only for the injection of infinitesimal small bubbles. Further study of the bubble dynamics for this case is anticipated to substantiate the validity range for the lumped analysis.

The system to be analyzed is, as shown in Fig. 11, the content of a vertical column of length $\ell$, connected to a reservoir at the top and closed at the bottom, except for the pipe through which gas is injected. The system has a constant volume, $V_S$, and is heated from the ambient.

Before injection of the gaseous component B, the system contains pure liquid of component A, subcooled or saturated, $T_o \leqslant T_A$, at the given system pressure. If the system is initially subcooled and the gas is soluble in the liquid, all the injected gas will go into liquid solution, causing heating rather than cooling until the system has reached a state of phase equilibrium given by the boiling curve $z_A = f(T)$. During continued injection two-phase equilibrium exists. The analysis therefore falls into two parts, namely, gas injection with liquid phase present only, and gas injection with two-phase equilibrium. For the cases of an initially saturated state of the liquid, or for zero liquid solubility of the injected gas, phase equilibrium exists from the start, and the first part of the analysis does not apply.

b. Gas Injection with Liquid Phase Present Only.—The analytical model is shown in Fig. 11. Gaseous component B with enthalpy $h''_{B,i}$ is injected at a constant mole-rate of $\dot{n}_B$ going into liquid solution, and liquid at a mole-rate of $\dot{n}'_{A,o}$ leaves the system. Further, heat flows from the ambient to the system at the rate of q.

With the general assumptions of a reversible isobaric process, and uniform temperature and composition throughout, the first law of thermodynamics leads to

$$n'_A\dot{h}'_A + n'_B\dot{h}'_B = \dot{n}_B h_{B,i} - \dot{n}'_{A,o}h'_{A,o} - \dot{n}'_B h'_B - \dot{n}'_A h'_A + q \qquad (10)$$

Continuity considerations give

$$\dot{n}'_A = -\dot{n}'_{A,o}$$

$$V_S = n'_A v'_A + n'_B v'_B.$$

Hence for $h'_A = h'_{A,o}$, a result of assuming uniform temperature, and with $\dot{h} = c\dot{T}$ and constant ambient heating rate, $q = \left(\frac{dT}{dt}\right)_o \cdot \Sigma\, c \cdot n$, Eq. (10) becomes

$$\frac{dT}{dt} = \frac{\dot{n}_B(h_{fg,B} + \Delta h_B)}{n'_A c'_A + n'_B c'_B} + \left(\frac{dT}{dt}\right)_o, \tag{11}$$

where the enthalpy change, $\Delta H_B = h''_{B,i} - h''_B$, of the gas when cooled from the injection temperature to the system temperature is assumed constant. This will be true for small temperature changes in cryogenic systems if the initial gas temperature is that of the ambient.

For small values of time, or as long as the integrated mass of injected and condensed gas contributes little to the heat capacity of the system, i.e., $n'_A c'_A \gg n'_B c'_B$, the quantity $n'_B c'_B$ can be neglected and $V_s \cong n'_A / v'_A$. Substituting further $\dot{n}_B = \dot{V}_B / v''_B$, Eq. (11) becomes

$$\frac{dT}{dt} = \frac{v'_A \dot{V}_B}{v''_B V_S}\left[\frac{h_{fg,B}}{C'_A} + \frac{\Delta h_B}{C'_A}\right] + \left(\frac{dT}{dt}\right)_o = C_1 \tag{12}$$

indicating a constant heating rate. Integration with the initial condition, $T = T_o$ for $t = o$, gives

$$T = T_o + C_1 t \tag{13}$$

Equation (13) describes the system temperature until the phase-equilibrium composition, $z_A(T_1)$, in the liquid is reached at time $t_1$. The temperature-composition relation during this process is determined as follows:

$$n'_B = \dot{n}_B t$$

$$\frac{n'_B}{n'_A} = \frac{1 - z_A}{z_A}$$

$$T = T_o + C_1 \left(\frac{v''_B}{v'_A}, \frac{V_s}{\dot{V}_B}\right) \frac{1 - z_A}{z_A} \tag{14}$$

Simultaneous solution of Eq. (14) and the equation for the boiling curve, $z_A = f(T)$, permit determination of the temperature at state 1, at which phase equilibrium is reached. The process from the initial state 0 to state 1 is schematically shown in Fig. 12.

Finally the time, $t_1$, for this part of the injection process can be obtained from Eq. (13).

In most practical cases the heating rate will be high. State 1 will fall near saturation for pure A and the time $t_1$ will be small. Further, injection cooling is normally started when the liquid to be cooled is already at saturation temperature.

c. Gas Injection with Two-Phase Equilibrium.—The analytical model for this case is shown in Fig. 13. Gas at the constant rate, $\dot{n}_B$, is injected at the lower end of the column of vertical height $\ell$, comprising the system. Immediately upon entering the system the gas comes to thermal and thermodynamic equilibrium with all the liquid and the gas presently in the system. This process is associated with evaporation of liquid component A and condensation of gas component B resulting in a given equilibrium gas composition, $x_A(T)$, and liquid composition, $z_A(T)$, corresponding to the system temperature T.

Depending on the velocity and composition of the gas rising through the system due to buoyancy, a variable hold-up volume, $V_G$, of gas must be considered. With the stipulation of constant system volume, the mass of liquid in the system is thus variable, accounted for by the flow rate $\dot{n}'_{A,i}$. Thus in the initial stage of the injection transient, liquid will leave the system until a certain quasi-steady hold-up volume of gas has built up. Following this stage the changes in gas volume are small until injection terminates and liquid of component A flows back from the reservoir to fill up the system. The temperature of this liquid will be that of the reservoir since free mixing can take place here. For very high rates of gas injection, liquid exchange with the reservoir would be of significance for lowering of system temperature. Such cases will not be considered here, where further the analysis is restricted to the above mentioned quasi-steady state.

For the general assumptions of an isobaric reversible process with uniform temperature and composition throughout each phase, and ignoring the heat capacity of the gas when it has been cooled to the system temperature, the first law of thermodynamics for the system in Fig. 13 becomes:

$$\begin{aligned} n'_A\dot{h}'_A + n'_B\dot{h}'_B &= (\dot{n}'_{A,i}h'_{A,i} - \dot{n}''_Ah''_A - \dot{n}'_Ah'_A) \\ &\quad - (\dot{n}''_Bh''_B + \dot{n}'_Bh'_B) + \dot{n}_Bh''_{Bi} + q, \end{aligned} \tag{15}$$

where the heat of mixing, surface effects, and kinetic and potential energy changes have been neglected. The equation of continuity gives:

$$\dot{n}'_A = \dot{n}'_{A,i} - \dot{n}''_A \tag{16}$$

$$\dot{n}'_B = \dot{n}_B - \dot{n}''_B \tag{17}$$

The condition of constant system volume becomes:

$$V_S = V_G + V_\ell = V_G + (n_A'v_A' + n_B'v_B'), \tag{18}$$

and finally by definition of composition in connection with phase-equilibrium requirements,

$$\frac{n_B''}{n_A''} = X = \frac{1 - x_A}{x_A} = f_1(T) \tag{19}$$

$$\frac{n_B'}{n_A'} = Z = \frac{1 - z_A}{z_A} = f_2(T). \tag{20}$$

Since the enthalpy flux due to inflow of liquid to the system is small, it will be assumed that $h_{A,i}' \cong h_A'$. With $\dot{h} = c\dot{T}$ and constant heating rate from the ambient, $q = (dT/dt)_o \cdot \Sigma\, c \cdot n$ and with Eqs. (16), (17), and (20), Eq. (15) becomes

$$\frac{dT}{dt} = \frac{1}{n_A'c_A'\left[1 + Z\,\frac{c_B'}{c_A'}\right]} \left[ - h_{fgA}\dot{n}_A'' + (\dot{n}_B - \dot{n}_B'')h_{fgB} + \dot{n}_B\Delta h_B \right] + \left(\frac{dT}{dt}\right)_o \tag{21}$$

where as in the previous section $\Delta h_B = h_{Bi}'' - h_B''$ is assumed constant. Equation (21) is further simplified in terms of the nondimensional temperature, $\theta = (T-T_B)/(T_A-T_B)$, by introducing Eq. (17) and the property groups defined in the nomenclature by capital letters,

$$\frac{d\theta}{dt} = E\,\frac{\dot{n}_B}{n_A'}\,\frac{1}{[1 + KZ]} \left[ - \left[ \frac{\dot{n}_A''}{\dot{n}_B''} + F \right] \frac{\dot{n}_B''}{\dot{n}_B} + F + C \right] + B. \tag{22}$$

Differentiating Eq. (20) and combining with Eq. (17) gives

$$Z\,\frac{\dot{n}_A'}{\dot{n}_B} + \dot{Z}\,\frac{n_A'}{\dot{n}_B} + \frac{\dot{n}_B''}{\dot{n}_B} - 1 = 0. \tag{23}$$

In addition to Eqs. (22) and (23), one more equation will be derived from the condition of constant system volume by evaluating the hold-up time for the gas in the system. The determination of the hold-up volume of gas in the system is subject to considerable uncertainty, and it can be accurately determined only

from full knowledge of bubble size, motion, and possible coalescence in connection with the fluid-flow pattern in the surrounding liquid. This type of data can be determined only by an experiment and the desirability of such physical measurements is indicated. However, a reasonably accurate estimate can be made based on the following reasoning. Let the gas bubbles rise through the liquid with an average velocity U. Knowing the vertical height, $\ell$, of the system, an average hold-up time can be defined as $\ell/U$. When a quasi-steady state has been reached, where gas phase is also leaving the system,

$$V_G = \dot{V}_G \frac{\ell}{U} = (v_A'' \dot{n}_A'' + v_B'' \dot{n}_B'') \frac{\ell}{U}. \tag{24}$$

Assuming the gas phase to be a mixture of ideal gases, $v_A'' = v_B'' = v''$, Eq. (24) gives with Eq. (18)

$$G\left(1 + \frac{\dot{n}_A''}{\dot{n}_B''}\right) \frac{\dot{n}_B''}{\dot{n}_B} + N(1 + ZL) \frac{n_A'}{\dot{n}_B} = 1. \tag{25}$$

Differentiating Eq. (19) and using again the assumed constant hold-up time $\ell/U$ for evaluating $n_B''/\dot{n}_B''$,

$$\frac{\dot{n}_A''}{\dot{n}_B''} = \frac{1}{X} - \frac{\dot{X}}{X^2} \frac{\ell}{U}. \tag{26}$$

Substituting Eq. (26) into Eq. (22) and (25), these equations with Eq. (23) give the formulation of the transient cooling in the form of the following three nonlinear coupled ordinary differential equations in the variables $\theta$, $(n_A'/\dot{n}_B)$ and $(\dot{n}_B''/\dot{n}_B)$:

$$\frac{d\theta}{dt} = \frac{E}{\left(\frac{n_A'}{\dot{n}_B}\right)} \frac{1}{1 + KZ} \left[ - \left( \frac{1}{X} - \frac{\dot{X}}{X^2} \frac{\ell}{U} + F \right) \left( \frac{\dot{n}_B''}{\dot{n}_B} \right) + F + C \right] + B \tag{27}$$

$$Z \left( \frac{\dot{n}_A'}{\dot{n}_B} \right) + \dot{Z} \left( \frac{n_A'}{\dot{n}_B} \right) + \left( \frac{\dot{n}_B''}{\dot{n}_B} \right) - 1 = 0 \tag{28}$$

$$G \left[ 1 + \frac{1}{X} - \frac{\dot{X}}{X^2} \frac{\ell}{U} \right] \left( \frac{\dot{n}_B''}{\dot{n}_B} \right) + N(1 + LZ) \left( \frac{n_A'}{\dot{n}_B} \right) = 1, \tag{29}$$

where the compositions are functions of temperature as given by the equilibrium characteristics of the binary mixture. The initial conditions are

$$t = 0$$

$$n'_A = n_{A,o} \qquad n'_B = n_{B,o} \tag{30}$$

$$\theta = \theta_o.$$

The assumption of a constant average gas velocity, U, upwards through the system is an idealization which in part can be justified by the general lumped approach for the present analysis. When the injected gas appears in discrete bubbles having little or no mutual interference, the velocity can be evaluated as the terminal velocity for the rise of single bubbles. For the case of cryogenic temperatures, U as a function of bubble size has been discussed by Clark, et al.[12] When the bubble population becomes greater mutual interference starts and greater velocities result due to strong liquid currents set up by the lifting action of the bubbles. As discussed by Morgan and Brady,[13] this region of mutual interference is characterized by ratios of vapor volume to total volume in the range 0.12 to 0.55. Above this range the bubble population is so high and coalescense so pronounced that large cylindrical bubbles or gas slugs form (Taylor bubbles), resulting in lower average gas velocities and geysering effects.

In view of the particular application of gas injection discussed here, only the regions of no or little mutual interference between the bubbles have interest and the velocity selected must be checked for consistency with the actual gas volume found.

d. Solutions.—The analytical model discussed above for gas injection with phase equilibrium resulted in the general formulation by Eqs. (27), (28), (29), and (30). While exact solution of the cooling transient is possible only by numerical calculation or the use of an analog computer, the subsequent discussion will be limited to the following cases:

(1) Asymptotic Solutions
(2) Approximate Transient Solution
    (a) Finite Liquid Solubility of the injected gas
    (b) Zero liquid solubility of the injected gas.

To permit analytical treatment the phase equilibrium data will further be approximated linearly in terms of the nondimensional temperature, $\theta = (T-T_B)/(T_A-T_B)$. Any higher-order approximation does not seem justified, since the region of interest is dilute binary solutions of B (injected gas) in A (liquid to be cooled). With reference to the tentative equilibrium diagram in Fig. 12, the following expressions result:

$$x_A = \theta \tag{31}$$

$$z_A = \epsilon(\theta - \theta_z), \tag{32}$$

where

$$\epsilon = \frac{T_A - T_B}{T_A - T_z}$$

$$\theta_z = \frac{T_z - T_B}{T_Z - T_B} = \frac{\epsilon - 1}{\epsilon}$$

(1) Asymptotic solution $\theta_\infty$.—When the system heating due to gas enthalpy flux and external heat transfer balances system cooling due to liquid evaporation, a steady state exists, and $\theta = \theta_\infty$ = constant. This idealized condition will exist for t approaching infinity to a good approximation if the reservoir above the system is large and free convective exchange of fluid between system and reservoir is suppressed. The latter implies further that only liquid of component A will enter the system.

It then follows from Eqs. (19) and (17) that

$$\frac{\dot{n}''_B}{\dot{n}''_A} = X$$

$$\frac{\dot{n}''_B}{\dot{n}_B} = 1$$

and Eq. (27) reduces to

$$\frac{d\theta}{dt} = A \frac{1 + LZ}{1 + KZ} \frac{-\frac{1}{X} + C}{1 - G\left(1 + \frac{1}{X}\right)} + B = 0 \qquad (33)$$

Substituting the linear equilibrium approximations, Eqs. (31) and (32), Eq. (33) becomes:

$$\alpha_1 \theta^2 + \alpha_2 \theta + \alpha_3 = 0, \qquad (34)$$

where

$$\alpha_1 = \epsilon \left[ (1 - L)(1 + C) + \frac{B}{A} (1 - K) \right]$$

$$\alpha_2 = - \left[ \epsilon(1 - L)(1 + 2C) - (1 + C) + \frac{B}{A} [\epsilon(1 - K)(2 - G) - 1] \right]$$

$$\alpha_3 = C [\epsilon(1 - L) - 1] + \frac{B}{A} (1 - G) [\epsilon(1 - K) - 1].$$

The property groups given by capital letters are listed in the nomenclature, and can be taken constant, when moderate changes in system temperature result.

The asymptotic value of system temperature, $\theta_\infty$, is the root of Eq. (34) in the interval $0 \leqslant \theta_\infty \leqslant 1$, and the highest attainable liquid subcooling for gas injection thus becomes:

$$\Delta T_{sub} = T_A - T_\infty = (T_A - T_B)(1 - \theta_\infty).$$

For the special case of zero liquid solubility of the injected gas, $z_A = 1$, Eq. (34) simplifies to

$$\theta_\infty = \frac{\frac{B}{A}(1 - G) + C}{1 + \frac{B}{A} + C}. \tag{35}$$

(2) Approximate transient solutions.—

(a) Finite liquid solubility of the injected gas.—An approximate solution in closed form can be obtained by the following simplifying assumptions:

$$\dot{n}'_A Z \ll n'_A \dot{Z} \tag{36}$$

$$V_G = V_{G,\infty} = \text{constant} \tag{37}$$

$$\frac{\dot{n}''_B}{\dot{n}''_A} = X. \tag{38}$$

The physical interpretation of Eq. (36) when compared with the time derivation of Eq. (20) is that the time rate of change of component B in the liquid phase is due mainly to the rate of change of composition, while the contribution from changes in the amount of liquid component A in the system is small. The assumption in Eq. (37) of constant hold-up volume of gas equal to that in the asymptotic stage of injection is probably not conservative but is motivated by the compensating effects determining this volume. In the first period of gas injection and when a quasi-steady state has been attained, i.e., when gas phase is also leaving the system, the main part of the injected gas goes into liquid solution while the gas phase will be very rich in component A and thus take up a large volume. Later, this relation will change and when the asymptotic stage is approached all the injected gas will remain in the gas phase, which, however, will now be less rich in component A and thus take up a comparatively smaller volume. Finally, the simplification introduced by Eq. (38) may be interpreted as neglecting any mass exchange between the rising gas phase and the surrounding liquid following the initial instantaneous equilibrium attained at the moment of injection. It is worth noting that this assumption clearly loses its physical validity if applied in determining the variable hold-up volume of gas, since this as seen from Eq. (29) can take arbitrary high values when $x_A$ is close to 1.0. This would be the case, for example, if the

initial condition for gas injection was saturated pure liquid of component A.

Introducing the assumptions in Eqs. (36), (37), and (38) into the general formulation, Eq. (28) becomes:

$$\frac{\dot{n}''_B}{\dot{n}_B} = 1 - \frac{n'_A}{\dot{n}_B}\dot{Z},$$

and Eq. (29) gives:

$$\frac{\dot{n}_B}{n'_A} = \frac{\dot{V}_B}{V_S}\frac{v'_A}{v''}\frac{1 + LZ}{1 - G\left(1 + \frac{1}{X_\infty}\right)},$$

where $X_\infty = (1 - \theta_\infty)/\theta_\infty$ according to Eqs. (19) and (31). Substituting the above results into Eq. (27) and noting that

$$\dot{Z} = \frac{\partial}{\partial t}\left(\frac{1 - z_A}{z_A}\right) = -\frac{1}{z_A^2}\left(\frac{\partial z_A}{\partial \theta}\right)_p \frac{d\theta}{dt},$$

the following results:

$$\left[1 + \frac{\left[\frac{1}{X} + F\right]}{1 + KZ}\frac{E}{z_A^2}\left(\frac{\partial z_A}{\partial \theta}\right)_p\right]\frac{d\theta}{dt} = A\cdot\frac{1 + LZ}{1 + KZ}\frac{-\frac{1}{X} + C}{1 - G\left(1 + \frac{1}{X_\infty}\right)} + B \qquad (39)$$

In view of the assumption of constant hold-up volume of gas, it does not seem justified to retain the volume and heat capacity correction terms in Eq. (39); hence $(1 + KZ) \cong 1$ and $(1 + LZ) \cong 1$. Introducing this and the linear equilibrium approximations, Eqs. (31) and (32), Eq. (39) becomes:

$$\frac{\epsilon\theta^3 + (1-3\epsilon)\theta^2 + \left[\frac{\epsilon-1}{\epsilon}(3\epsilon-1) - \epsilon E(1-F)\right]\theta - \left[\frac{(\epsilon-1)^2}{\epsilon} + EF\right]}{\epsilon\left(\theta - \frac{\epsilon-1}{\epsilon}\right)^2\left[(1+D_1)\theta - D_1\right]}\cdot\frac{d\theta}{dt} = A_1 \qquad (40)$$

where $A_1 = A/[1-G(1+1/X_\infty)]$ and $D_1 = B/A_1 + C$. Equation (40) can be integrated after partial fraction expansion, and for large values of time $\theta \to D_1/(1+D_1)$, which deviates slightly from the exact asymptotic value, $\theta_\infty$ given by Eq. (34).

If, in addition, dilute solutions are considered (i.e., $z_A \cong 1$), Eq. (39), in conjunction with Eqs. (31) and (32), reduces to

$$\frac{[1 - \epsilon E(1-F)]\theta - [1+\epsilon EF]}{(1+D_1)\theta - D_1} \cdot \frac{d\theta}{dt} = A_1,$$

and integration yields:

$$\left[\frac{1}{1 + D_1} + \frac{\epsilon E}{1 - \epsilon E(1-F)}\right] \ell n \frac{\theta_o - \theta_\infty}{\theta - \theta_\infty} - [\theta_o - \theta] = \frac{(1+D_1)A_1 t}{1 - \epsilon E(1-F)}, \quad (41)$$

where

$$\theta_\infty = \frac{D_1}{1 + D_1},$$

identical with the expression in Eq. (35). This solution, though not conservative, predicts approximately the cooling transient. The effect of liquid solubility of the gas is found in the factors $\epsilon$ and F, and will be discussed in a subsequent section.

(b) Zero liquid solubility of the Injected Gas.—When the injected gas is not soluble in the liquid phase, $z_A = 1$, $\epsilon = 0$, and phase equilibrium exists from the moment of injection. Hence Eq. (41) holds for $\epsilon = 0$, reducing to

$$\frac{1}{1 + D_1} \ell n \frac{\theta_o - \theta_\infty}{\theta - \theta_\infty} - [\theta_o - \theta] = (1+D_1)A_1 t, \quad (42)$$

where

$$\theta_\infty = \frac{D_1}{1 + D_1}.$$

The solution in Eq. (42) represents an extension of the solution given on p. 45 of Ref. 1, in accounting for the enthalpy flux of injected gas and the presence of rising bubbles, decreasing the system heat capacity. However, the temperature dependency of the property group A has been ignored in Eq. (42), assuming the use of an average value.

e. Discussion of Solutions. Effect of Gas Solubility.--It appears from the physical model introduced in describing the injection process that the maximum attainable subcooling, determined by the asymptotic temperature, $\theta_\infty$, from Eq. (34), is insensitive to the final liquid composition. This follows from the assumption that only liquid of component A flows into the system, making up for the evaporation of this component in the asymptotic steady state. Hence all the injected gas remains in the gaseous phase. As seen from Eq. (33), the effect of solubility enters only in the correction term, (1 + LZ)/(1 + KZ), to the specific volume and specific heat of the liquid in the system. Omission of this term and use of Eq. (35) will introduce only a minor error, especially

if the final liquid concentration of component B is low or the properties of component A and B are nearly the same.

While the asymptotic temperature thus is essentially unaffected by a finite gas solubility, this becomes effective in decreasing the cooling rate. Solving Eq. (41) for time, t, gives the following expression:

$$t = \alpha_4 + \alpha_5 \epsilon + \alpha_6 \epsilon F,$$

where the slope of the boiling curve, $\epsilon$, and the ratio of heats of evaporation, F, are the only factors that depend on solubility. The coefficients $\alpha_4$, $\alpha_5$, and $\alpha_6$ are functions of all other system parameters and are positive. Zero solubility, $\epsilon = 0$, gives a minimum cooling time, $t = \alpha_4$, as obtained by Eq. (42). Increasing $\epsilon$ and F gives increasing cooling times, since, respectively, the solubility increases as the cooling proceeds and the temperature drops, and the enthalpy flux due to condensation of the injected gas increases. Appendix II gives an evaluation of the effect of solubility based on a sample calculation for a hydrogen-helium system.

## 2. LOX-SYSTEMS COOLED BY He-INJECTION

Oxygen-helium systems at states considerably above the critical state of helium are characterized by very low solubility of helium in liquid oxygen. Data[14] indicate that the assumption of zero liquid solubility, $z_A = 1$, is justified throughout the range of interest.[15] In this case the transient cooling can be described by the solution given above in Eq. (42), and the asymptotic temperature is determined by Eq. (35).

In evaluating the characteristics of injection cooling applied to a given system, two aspects are of primary interest, namely, the lowest attainable temperature, $T_\infty$, and the time required to reach some specified temperature $T_2 > T_\infty$. The actual cooling curve is of secondary importance.

Such sample calculations are given in Appendix I for the particular He-cooled LOX system discussed previously,[1] indicating that $T_\infty = 170.2°R$, and that 3.17 min of gas injection at a rate of 70 scfm brings the system temperature to $T_2 = 171.5°R$, equivalent to 90% of the possible sub-cooling, $T_o - T_\infty$. This result does not differ significantly from that obtained previously (Ref. 1, Fig. 81, indicates $T_2 = 174.4°R$ after 3.17 min), where two effects were omitted, namely, the presence of rising bubbles reducing the system heat capacity and the enthalpy flux of the injected gas. The two effects have, however, a compensating influence on the results.

The agreement between experimental results and the predictions from the lumped analysis indicates that this adequately describes the average temperature response to the injection of a nonsoluble gas.

## 3. $LH_2$-SYSTEMS COOLED BY He-INJECTION

The critical state of hydrogen, and in general the states at which liquid ($LH_2$) is normally being handled, are much closer to the critical state of helium than is the case for oxygen as discussed above. Therefore, higher solubility of He in $LH_2$ can be anticipated, and the assumption of zero liquid solubility is no longer valid.

In the literature search only one source[16] was discovered presenting experimental data for phase-equilibrium in helium-hydrogen systems. The data cover liquid and gas compositions for systems at 17.40°K, 20.39°K, and 21.80°K for pressures up to about 500 psia and indicate solubilities up to 3.5 mole-% in this range. Further, it was shown that the solute (helium) obeyed Henry's Law in the pressure range studied, while there were considerable deviations from Raoult's Law for the solvent.

To demonstrate the effect of a sizable liquid solubility of the injected gas, the tentative hydrogen-helium equilibrium diagram in Fig. 12 for an arbitrary selected system pressure of 120 psia was prepared, assuming ideal gas/ideal solution. The dew-curve and boiling-curve were approximated by straight lines as shown in Fig. 12 such that the asymptotic temperature, $\theta_\infty$, could be found by Eq. (34) or (35) and the transient cooling by Eq. (41). Such sample calculations are given in Appendix II for a system identical to that discussed previously[1] with respect to geometry, ambient heating and helium injection rate (70 scfm), but it is assumed that the system initially contains saturated liquid hydrogen at the system pressure 120 psia. It is found that a maximum subcooling of 0.96°F can be obtained under these circumstances and 90% of this is obtained after 0.69 min of gas injection. Increasing solubility increases this cooling time. Further, a subcooling of 4.56°F should be attainable if the helium were pre-cooled to system temperature, according to this analysis.

From the discussion of the general characteristics of injection cooling (Ref. 1, p. 47), it was shown that the maximum attainable subcooling for an adiabatic system decreased with the absolute temperature, and that the cooling rate increased. Irrespective of system components, the obtainable subcooling will thus decrease with decreasing absolute temperature of the system. This explains in part the small subcoolings observed for He-injection in $LH_2$. However, the limitation of the lumped analysis in implying instantaneous equilibrium may well be significant. A final analysis of injection of a soluble gas into a volatile liquid is therefore proposed to include a detailed study of the rates of mass and heat transfer associated with finite initial bubble size of the injected gas.

## B. Bubble Dynamics of a Distributed System

### 1. HEAT AND MASS DIFFUSION IN A MOVING MEDIUM WITH TIME-DEPENDENT BOUNDARIES

The equation for heat conduction in a moving, inviscid fluid with given motion of the boundaries can be expressed as

$$\alpha\nabla^2 T - u(\bar{r},t) \text{ grad } T - \frac{\partial T}{\partial t} = 0 \qquad (43)$$

where $T(\bar{r},t)$ is the temperature and $u(\bar{r},t)$ the local velocity of the fluid, $\bar{r}$ being the radius vector at $(x,y,z)$ and given by $\bar{r} = \bar{r}_o(t)$ as a known function of time.

The following boundary conditions will be considered.

$$T = 0; \text{ or } \frac{\partial T}{\partial n} = 0 \qquad \text{for } \bar{r} = \bar{r}_o(t) \qquad (44)$$

where $\bar{r}_o$ is the radius vector of the moving boundary. Forster[17] has presented a method to find the analytical solution to this problem from the solutions for the associated problem of diffusion in a stationary medium with stationary boundaries. Since the same method will be applied in the following analysis, it is appropriate to describe the approach briefly here.

If $\Delta t$ is sufficiently small, one can assume that the boundary moves, as shown in Fig. 14, from A to C to B instead of proceeding from A to B directly. When the boundary moves from A to C and fluid particles move from A' to C', the velocity $u(\bar{r},t)$ is everywhere zero because $\bar{r}_o$ remains constant. Therefore between A and C, A' and C', Eq. (43), becomes

$$\alpha\nabla^2 T - \frac{\partial T}{\partial t} = 0 \qquad (45)$$

Between times t and $t + \Delta t$ it is assumed that $T(\bar{r},t)$ is known and $T(\bar{r},t + \Delta t)$, that is, the solution of Eq. (45) for $t + \Delta t$, is desired. Each fluid particle is then shifted instantaneously from C to B, from C' to B', whereby the redistribution of temperature due to convection effect is achieved, and each fluid particle attains the position it should occupy in accordance with the prescribed motion.

These steps can be mathematically performed by the use of Green's function for Eq. (45) for the domain bounded by AC, which may be denoted by $G(\bar{r},\bar{r}',t)$. Then the temperature at point C' is

$$\Theta(\bar{r},t+\Delta t) = \int_{\bar{r}_o(t)}^{\infty} T(\bar{r}',t)G(\bar{r},\bar{r}',t)dr' \qquad (46)$$

where dr' is the volume element (dx'dy'dz') at $\bar{r}$. The displacement $\Delta\bar{r}$ of the fluid particle at $\bar{r}$ can be evaluated as the local velocity $\bar{u}(\bar{r},t)$ of the fluid is given; then as each fluid particle is shifted by $\Delta\bar{r}$ from the points C' to B', the temperature at B' is given from Eq. (46) by $\Theta[(\bar{r}-\Delta\bar{r}),\ t+\Delta t]$ or explicitly

$$T(\bar{r},t+\Delta t) = \int_{\bar{r}_o(t)}^{\infty} T(\bar{r}',t)G[(\bar{r}-\Delta\bar{r}),\ \bar{r}',\Delta t]\,dr' \qquad (47)$$

Equation (47) is the exact solution of Eq. (43) for the approximating boundary motion A to C to B. Therefore, given an initial temperature distribution $T(\bar{r},0)$, the time interval t may be subdivided into n sub-intervals and the exact solution of the equation is obtained by repeated application of Eq. (47) to the n sub-intervals.

For the fluid motion represented by $f_2$ in Fig. 14, a related formula may be derived by performing the operation given by Eq. (46) previous to Eq. (47) in reverse order, i.e., taking the path from A to D to B, and from A' to D' to B'. $T_1^n(\bar{r},t)$ then is the solution of Eq. (43) for the path $f_1$ and $T_2^n(\bar{r},t)$ that for the path $f_2$ both for time t in n intervals. Both $T_1$ and $T_2$ tend to the solution of Eq. (43) for boundary motion $\bar{r}_o(t)$, since both $f_1$ and $f_2$ tend to $\bar{r}_o(t)$. Therefore the temperature of the fluid particle for a given motion is intermediate between $T_1^n$ and $T_2^n$ if the path of every fluid particle is always intermediate between $f_1$ and $f_2$.

## 2. APPLICATION OF THE THEORY IN IV-B-1 TO BUBBLE GROWTH

(a) Bubble Growth in a Boiling Liquid.—At the asymptotic stage, the growth of a bubble is governed by the rate at which latent heat of vaporization can be supplied at the bubble surface. The governing differential equation is identical with Eq. (43) with $T(\bar{r},t)$ representing temperature. Since the latent heat of vaporization supplied to the bubble surface from the vapor phase is negligible compared with that supplied from the surrounding liquid, the bubble surface may be regarded as a heat sink, thermally insulated on the vapor side, continuously absorbing heat from the surrounding fluid. The approximate Green's function to be used can be found in Ref. 18, p. 368. The temperature increment at the bubble surface of radius R(t) at time t due to an amount of heat $\rho'C'dQ(y)$ liberated on the bubble of radius R(y) at time y may be obtained from Eq. (16) on p. 368 of Ref. 18 by substituting $r' = a = R(\xi)$, $r = R(\xi)$, $t = t - y$, and $h = 0$:

$$dT_s = \frac{dQ_T(y)}{4\pi\sqrt{\pi\alpha}\sqrt{t-y}\,R^2(\xi)}\left[1 - \frac{\sqrt{\pi\alpha(t-y)}}{R(\xi)}e^{\frac{\alpha(t-y)}{R^2(\xi)}}\operatorname{erfc}\frac{\sqrt{\alpha(t-y)}}{R(\xi)}\right] \qquad (48)$$

where

$Q_T(y)$ = strength of an instantaneous point sink of heat

$\xi$ = a variable ranging from time y to time t

y = a time between t = 0 and t = t

$R(\xi)$ starts at R(y) and grows to R(t).

An approximate mean value for $R(\xi)$ is calculated by Forster[19] to be

$$R(\xi) = \sqrt{R(y)\, R(t)} \tag{49}$$

If the radius R(y) of the bubble increases by dR(y), an amount of heat

$$\rho' C' dQ_T(y) = - 4\pi R^2(y) h_{fg} \rho'' \dot{R}(y) dy \tag{50}$$

is absorbed constituting a distributed spherical heat sink. As discussed in Ref. 17, the second term in the bracket in Eq. (48) is small when the contribution of $dT_s$ is large and the contribution of $dT_s$ is small by the time the second term becomes important. Therefore the combination of Eqs. (48), (49), and (50) gives:

$$dT_s = \frac{h_{fg} \rho'' R(y) \dot{R}(y) dy}{C' \rho' \sqrt{\pi\alpha}\, \sqrt{t-y}\, R(t)} \tag{51}$$

Integration of Eq. (51) gives the temperature of the bubble surface at time t:

$$T_s = - \frac{h_{fg} \rho''}{C' \rho' \sqrt{\pi\alpha}} \int_0^t \frac{R(y) \dot{R}(y) dy}{\sqrt{t-y}\, R(t)} + T_\infty \tag{52}$$

where $h_{fg}$ is the latent heat of vaporaization, $\rho''$ and $\rho'$ the molal density of vapor or liquid, respectively, c', the molal specific heat of liquid. It is justified to express the bubble growth as

$$R(t) = 2\lambda \sqrt{\alpha t} \tag{53}$$

Substituting R(t), R(y), and $\dot{R}(y)$ obtained from Eq. (53) into Eq. (52), one obtains $\lambda$, the coefficient of the bubble growth, as follows

$$\lambda = \frac{\rho' c' \sqrt{\pi}}{2 \rho'' h_{fg}} (T_\infty - T_s) \tag{54}$$

where $T_\infty - T_s$, the effective superheat, is identical to the liquid superheat, since in this case $T_s$ is the saturation temperature of the liquid. The bubble growth then can be written as:

$$R(t) = \frac{\rho' c' (T_\infty - T_s)}{\rho'' h_{fg}} \sqrt{\pi \alpha t} \tag{55}$$

Results obtained by this approximation give good agreement with the experimental results by Dergarabedian,[20] Griffith,[21] and the theoretical results by Scriven.[22] These results may also be applied to predict the rate of bubble growth in cryogenic liquids.

(b) Bubble Growth in a Binary System.—If the liquid in which the bubble grows is a mixture of two components, the rate of bubble growth at the asymptotic stage is controlled by the transport of heat and mass from the liquid to the bubble surface. By assuming the existence of a thermodynamic equilibrium at the bubble surface during the bubble growth, Scriven[22] obtained exact solutions in nonclosed forms to predict the rate of the growth in binary liquid mixtures. Benjamin and Westwater[23] conducted experiments to measure the growth rate of bubbles in mixtures of water and ethylene glycol. The agreement between theory and experiment over the entire range of concentrations is good qualitatively.

However, the approximate solution can be found by applying the theory above. Equations for both heat and mass transfer in the binary mixture are identical with Eq. (43). One may consider the mechanism of the bubble growth as two simultaneous processes: (i) the bubble surface may be regarded as heat sink, thermally insulated on the vapor side, continuously absorbing heat from the surrounding liquid; (ii) the bubble surface may be regarded as mass sink continuously absorbing mass only from the surrounding liquid and diffusing it into the bubble space after the liquid is vaporized. Then the temperature of the bubble surface at time t can be expressed by Eq. (52). The concentration increment of the more volatile component B at the bubble surface of radius R(t) at time t due to an amount of mass $\rho' dQ_c(y)$ evaporated on the bubble of radius R(y) at time y may be expressed in the identical form as Eq. (48):

$$dz_{B,S} = \frac{dQ_c(y)}{4\pi \sqrt{\pi \alpha' (t-y)}\, R(\xi)} \left[1 - \sqrt{\pi}\, \frac{\sqrt{\alpha' (t-y)}}{R(\xi)}\, e^{\frac{\alpha' (t-y)}{R^2(\xi)}}\, \operatorname{erfc} \frac{\sqrt{\alpha' (t-y)}}{R(\xi)}\right] \tag{56}$$

where

$Q_c(y)$ = the strength of an instantaneous point sink of mass, $ft^3$

$z_{B,S}$ = concentration of the more volatile component B in the liquid phase expressed as mole fraction

If the radius R(y) of the bubble increases by dR(y), an amount of mass

$$\rho' dQ_c(y) = -4\pi R^2(y) \frac{dR(y)}{dy}\, dy \rho'' x_{B,S} \tag{57}$$

is absorbed constituting a distributed spherical mass sink. $x_{B,S}$ is the concentration of the more volatile component B in the gas phase at the bubble interface expressed as mole fraction.

If the second term in the bracket in Eq. (56) is ignored as in case (a), the combination of Eqs. (49), (56), and (57) gives:

$$dz_{B,S} = - \frac{\rho'' R(y)\dot{R}(y)dy}{\rho' R(t)\sqrt{\pi \mathcal{D}'(t-y)}} x_B \tag{58}$$

Integration of Eq. (58) gives for the mole fraction of the component B in the liquid state at the bubble surface at time t:

$$z_{B,S} = - \frac{\rho'' x_{B,S}}{\rho' \sqrt{\pi \mathcal{D}}} \int_0^t \frac{R(y)\dot{R}(y)}{R(t)\sqrt{t-y}} dy + z_{B,\infty} \tag{59}$$

where $\mathcal{D}'$ is the mass diffusivity, and $z_{B,\infty}$ is the mole fraction of the more volatile component B in the liquid phase at a distance from the bubble.

By substituting Eq. (53) into Eq. (59), one obtains

$$z_{B,S} = - \frac{2\rho'' \lambda x_{B,S}}{\rho' \sqrt{\pi}} \sqrt{\frac{\alpha}{\mathcal{D}'}} + z_{B,\infty} \tag{60}$$

The equilibrium conditions existing on the bubble surface during its asymptotic growth gives a relationship between temperature and concentration at the bubble surface as:

$$x_{B,S} - x_{B,\infty} = \left(\frac{\partial x_A}{\partial T}\right)_p \left(T_{\infty,\text{sat.}} - T_s\right) \tag{61}$$

where $x_{B,\infty}$ is the vapor composition in equilibrium with liquid of composition $z_{B,\infty}$ at a distance from the bubble, and

$$z_{B,S} - z_{B,\infty} = \left(\frac{\partial z_A}{\partial T}\right)_p \left(T_{\infty,\text{sat.}} - T_s\right) \tag{62}$$

since $z_A = 1 - z_B$.

Substituting Eqs. (54) and (60) into Eq. (62) to eliminate $T_s$ and $z_{B,S} - z_{B,\infty}$, one obtains

$$\lambda = \frac{\sqrt{\pi}}{2} \frac{\rho' C'}{\rho'' h_{fg}} (T_\infty - T_{\infty,\text{ sat.}}) \frac{1}{1 + \frac{C'}{h_{fg}} \sqrt{\frac{\alpha}{\mathcal{D}'}} \frac{x_{B,S}}{\left(\frac{\partial z_A}{\partial T}\right)_p}} \tag{63}$$

The last factor in Eq. (63) can be considered the correction factor to the liquid superheat, $T_\infty - T_{\infty,sat.}$, which gives the effective superheat $T_\infty - T_S$ for bubble growth according to Eq. (54). For the one-component system, this factor is equal to unity and Eq. (63) reduces to Eq. (54). The gas composition $x_{B,S}$ is a function of the interface temperature $T_S$ and can be eliminated from Eq. (63) by Eqs. (61) and (54), resulting in a quadratic equation in $\lambda$.

The coefficient $\lambda$ of a bubble growth in the binary liquid mixtures of water and ethylene glycol is analyzed. The results agree very well with those predicted by Scriven.[22]

(c) Bubble Growth of Noncondensing Gas in Cryogenic Liquids.—The theory which is confirmed in the previous cases (a) and (b) is further extended to predict the growth rate of helium bubbles in the liquid oxygen or nitrogen. Equations for heat transfer in the liquids and mass transfer in the helium bubble can be expressed in the same form as Eq. (43). One may consider the mechanism of the bubble growth as two simultaneous processes: (i) the bubble surface may be regarded as a heat sink absorbing heat, thermally insulated on the vapor side, from the surrounding liquid oxygen; (ii) the bubble surface may be regarded as a mass source materially insulated on the liquid side, continuously diffusing gaseous oxygen into the bubble space occupied by the helium gas.

These two simultaneous processes are coupled by the equilibrium relation existing at the bubble surface.

The temperature of the bubble surface at time t is identical with Eq. (52). For the mass diffusion of gaseous oxygen or nitrogen into helium in the bubble space, the appropriate Green's function to be used can be found in Ref. 18, p. 367. The concentration increment of the gaseous oxygen or nitrogen at the bubble surface of radius R(t) at time t due to an amount of mass $\rho' dQ_M(y)$ evaporated on the bubble of radius R(y) at time y may be obtained from Eq. (10) on p. 367 of Ref. 18 by substituting $r' = a = R(\xi)$, $r = R(\xi)$, $t = t-y$, and $h = 0$:

$$dx_s = \frac{dQ_M(y)}{2\pi R^3(\xi)} \sum_{n=1}^{\infty} \frac{1 + [R(\xi)\gamma_n]^2}{[R(\xi)\gamma_n]^2} \sin^2 [R(\xi)\gamma_n] e^{-\mathcal{D}''\gamma_n^2(t-y)} + \frac{3dQ_y(y)}{4\pi R^3(\xi)} \qquad (64)$$

where the $\gamma_n$ are the positive roots of

$$[R(\xi)\gamma]\cot[R(\xi)\gamma] = 1 \qquad (65)$$

The roots of the transcendental Eq. (65) may be found from Table II on p. 492 of Ref. 18. $x_s$ is the concentration of the vaporized cryogenic materials at the bubble boundary expressed as mole fraction and $Q_M(y)$ the strength of an instantaneous point source of mass which refers to the cryogenic liquid in the problem.

With the substitution of the geometric mean radius expressed by Eq. (49) into Eq. (64), one obtains

$$dx_s = \frac{dQ_M(y)}{2\pi[R(y)]^{3/2}[R(t)]^{3/2}}\left[\frac{3}{2} + \sum_{n=1}^{\infty} e^{-\alpha\gamma_n^2(t-y)}\right] \tag{66}$$

By substituting the $\gamma_n$'s the second term in the bracket in Eq. (66) may be written as

$$\sum_{n=1}^{\infty} e^{-\mathcal{D}''\gamma_n^2(t-y)} = 1 + e^{-(4.49)^2\frac{\mathcal{D}''(t-y)}{R(t)R(y)}} + e^{-(7.73)^2\frac{\mathcal{D}''(t-y)}{R(t)R(y)}} + e^{-(10.9)^2\frac{\mathcal{D}''(t-y)}{R(t)R(y)}} + e^{-(14.07)^2\frac{\mathcal{D}''(t-y)}{R(t)R(y)}} + \text{-----} \tag{67}$$

Following Forster's[17] reasoning, Eq. (67) may be approximated by 1 as time increases.

As the radius R(y) of the bubble increases by dR(y), an amount of mass

$$\rho' dQ_M(y) = 4\pi R^2(y)\dot{R}(y)\rho'' \tag{68}$$

is generated constituting a distributed spherical mass source of gaseous oxygen or nitrogen to diffuse into the bubble space. Integration of Eq. (66) gives

$$x_s = \frac{10\rho''}{3\rho'} \tag{69}$$

For the sake of simplicity a linear approximation is assumed for the dew curve for the phase equilibrium of the helium-oxygen system according to Eq. (31). Hence

$$T_s = T_B + (T_A - T_B)x_s \tag{70}$$

and Eqs. (54), (69), and (70) then give:

$$\lambda = \frac{\sqrt{\pi}}{2}\frac{\rho'C'}{\rho''h_{fg}}(T_A - T_B)\left[\frac{T_\infty - T_B}{T_A - T_B} - \frac{10}{3}\frac{\rho''}{\rho'}\right] \tag{71}$$

In obtaining Eq. (69) by integration of Eq. (66), the initial bubble size was assumed zero. Considering a finite initial bubble size, $R_o$, Eq. (69) becomes

$$x_s = \frac{10}{3}\frac{\rho''}{\rho'}\left[1 - \left(\frac{R_o}{R(t)}\right)^{3/2}\right] \tag{72}$$

Hence $T_s$ cannot be considered constant, a necessary condition for the integration of Eq. (52) with the result of Eq. (54). For large values of time, however, $x_s$ approach the constant value given by Eq. (69), and Eq. (71) therefore gives an approximate expression for the coefficient, $\lambda$, of bubble growth for helium gas in liquid oxygen at temperature $T_\infty$.

## APPENDIX I

### SAMPLE CALCULATION FOR LOX-SYSTEM COOLED BY He-INJECTION

The data summarized below pertain to the example discussed in a previous study,[1] with the additional condition that the injected helium is initially at ambient temperature, about 200°C = 360°F above the system temperature.

$$T_o = 183.6°R$$

$$T_A = 184.4°R$$

$$T_B = 155.0°R$$

$$T_A - T_B = 29.4°R$$

$$\theta_o = (T_o - T_B)/(T_A - T_B) = 0.973$$

$$\delta_A = 1.8°F \text{ (mean value)}$$

$$V_S = 7.32 \text{ ft}^3$$

$$\dot{V}_B = 7.80 \text{ ft}^3/\text{min at } 3.1 \text{ ata}, 180°R$$

$$\left(\frac{dT}{dt}\right)_o = 1.3°F/\text{min}$$

Assuming an average gas velocity, U = 2 ft/sec, and with a total length of the LOX-line of 21 ft (the vertical height is 15 ft) the hold-up time becomes $\ell/U = 10.5$ sec. Hence

$$A = \frac{\delta_A}{T_A - T_B}\frac{\dot{V}_B}{V_S} = 0.0653 \text{ min}^{-1}$$

$$B = \frac{1}{T_A - T_B}\left(\frac{dT}{dt}\right)_o = 0.0442 \text{ min}^{-1}$$

$$C = \frac{\Delta h_B}{h_{fgA}} = \frac{c''_B \Delta T}{h_{fgA}} = \frac{5 \times 200}{1545} = 0.650$$

$$G = \frac{\ell}{U}\frac{\dot{V}_B}{V_S} = 0.187.$$

The asymptotic temperature is thus from Eq. (35)

$$\theta_\infty = \frac{B/A(1 - G) + C}{1 + B/A + C} = 0.516; \text{ or } T_\infty = 170.2°R,$$

whereby

$$A_1 = \frac{A}{1 - G(1 + 1/x_\infty)} = 0.1063,$$

and the transient cooling is given by Eq. (42)

$$\frac{1}{2.066} \ln \frac{0.973 - 0.516}{\theta - 0.516} - [0.973 - \theta] = 0.22\ t.$$

Assume 90% of the possible cooling is desired, i.e., $\theta_2 = 0.562$, or $T_2 = 171.5°R$. The time $t_2$ required to reach this value is from the above equation for the transient cooling for $\theta = \theta_2$, $t_2 = 3.17$ min.

## APPENDIX II

The data summarized below pertain to the system discussed previously[1] with respect to geometry, ambient heating, and injection rate (70 scfm, He), but assumes liquid hydrogen present at a pressure of 120 psia, and the injected helium initially at ambient temperature, about 300-30 = 270°C = 486°F above system temperature. Equilibrium data are tentative and taken from Fig. 12.

$$T_A = 54°R$$

$$T_B = 42°R$$

$$T_A - T_B = 12°R$$

$$T_z = -15°R$$

$$\epsilon = \frac{T_A - T_B}{T_A - T_z} = 0.174$$

$$\theta_z = \frac{T_z - T_B}{T_A - T_B} = \frac{\epsilon - 1}{\epsilon} = -4.75$$

$$\delta_A = \frac{h_{fgA} v'_A}{c'_A v''} = 5.9°F$$

$$V_S = 7.32\ ft^3$$

$$\dot{V}_B = 0.94\ ft^3/min \text{ at } 54°R, 120 \text{ psia}$$

$$\left(\frac{dT}{dt}\right)_o = 1.3°F/min$$

Because of the smaller volume of the injected gas, the bubble velocity is estimated to 1 ft/sec resulting in a hold-up time of $\ell/U = 21$ sec. Hence

$$A = \frac{\delta_A}{T_A - T_B} \frac{\dot{V}_B}{V_S} = 0.0556\ min^{-1}$$

$$B = \frac{1}{T_A - T_B} \left(\frac{dT}{dt}\right)_o = 0.108\ min^{-1}$$

$$C = \frac{\Delta h_B}{h_{fgA}} = 9.37$$

$$E = \frac{1}{T_A - T_B} \frac{h_{fgA}}{c'_A} = 2.16$$

$$F = \frac{h_{fgB}}{h_{fgA}} = 0.1$$

$$G = \frac{\ell}{U}\frac{\dot{V}_B}{V_S} = 0.045$$

$$K = \frac{c'_B}{c'_A} = 0.4$$

$$L = \frac{v'_B}{v'_A} = 1$$

$$M = \frac{v''}{v'_A}\frac{\ell}{U} = 1.75 \text{ min}^{-1}$$

$$N = \frac{v'_A}{v''}\frac{\dot{V}_B}{V_S} = 0.0257 \text{ min}^{-1}$$

$$A_1 = \frac{1}{1 - G(1 + 1/X_\infty)} = 0.126 \text{ min}^{-1}$$

$$D_1 = B/A_1 + C = 10.22$$

$$D = B/A + C = 11.31$$

Substitution into Eq. (34) gives:

$$0.203\,\theta^2 + 11.92\,\theta + 11.03 = 0,$$

or

$$\theta = \begin{cases} 0.918 \\ -59.52, \end{cases}$$

hence $\theta_\infty = 0.918$ and $\Delta T_{sub} = T_A - T_\infty = 0.96°F$, equivalent to a final liquid composition, $z_{A\infty} = 0.989$. For comparison $\theta_\infty = 0.912$ is obtained if Eq. (35) is used.

Assume 90% of the possible cooling is desired, i.e., $\theta_2 = 0.926$. The time, $t_2$, required to reach this value is obtained from Eq. (41) to $t_2 = 0.692$ min. The effect of finite solubility in terms of the parameters $\epsilon$ and F can be seen from the expression

$$t_2 = 0.0928 + 3.32\,\epsilon + 0.205\,\epsilon F,$$

obtained from Eq. (41) by substituting the above values for properties and initial and final temperatures. Increasing the solubility from zero by changing the slope, $\epsilon$, of the boiling curve from $\epsilon = 0$ to positive values

gives rapidly increasing cooling times, from $t_2 = 0.093$ min at $\epsilon = 0$ to $t_2 = 3.43$ min for $\epsilon = 1$ and $F = 0.1$. The cooling time also increases with increasing ratio of heat of evaporation, F, though less pronounced.

If the injected gas was precooled to system temperature, i.e., $C = 0$, $\theta_\infty = 0.62$ is found equivalent to a subcooling of 4.56°F.

## REFERENCES


1. Clark, J A., H. Merte, Jr., V. S. Arpaci, et al., Pressurization of Liquid Oxygen Containers, Univ. of Mich. ORA Report 04268-2-P, Ann Arbor, Nov., 1961.

2. Chang, Y., and N. W. Snyder, "Heat Transfer in Saturated Boiling," Preprint 104 presented at Third National Heat Transfer Conference, ASME-AIChE, August, 1959.

3. Vorishanskii, V. M., "An Equation Generalizing Experimental Data on the Cessation of Bubble Boiling in a Large Volume of Liquid," Zhurn. Tekh. Fiz., 26, 452 (1956). Translated in Soviet Physics-Technical Physics, 1, No. 2, 438, Am. Inst. of Phys., N.Y.

4. Zuber, N., "On the Stability of Boiling Heat Transfer," Trans.ASME, 80, 711 (April, 1958).

5. Usiskin, C. M., and R. Siegel, "An Experimental Study of Boiling in Reduced and Zero Gravity Fields," Trans. ASME, J. Heat Transfer, Series C, 83, 243 (Aug. 1961).

6. Bromley, L. A., "Heat Transfer in Stable Film Boiling," Chem. Eng. Prog., 46, 221 (1950).

7. Convair Astronautics Progress Report No. AE61-0871 of 5 Sept. 1961 (AF18(600)-1775), as modified by personal communication, W. B. Mitchell to J. A. Clark, WBM:JES:mas 595-1-16645 of 23 Oct. 1961.

8. Zuber, N., and M. Tribus, Further Remarks on the Stability of Boiling Heat Transfer, Rept. 58-5, Dept. of Engr., Univ. of California at Los Angeles, Jan. 1958.

9. Plesset, M. S., and S. A. Zwick, "Growth of Vapor Bubbles in Superheated Liquids," J. Appl. Phys., 25, 493-500 (1954).

10. Dergarabedian, P., "Observations on Bubble Growth in Various Superheated Liquids," J. Fluid. Mech., 9, 39-48 (1960).

11. Bird, R. B., W. E. Stewart, and E. N. Lightfoot, Transport Phenomena, John Wiley and Sons, Inc., 1960, p. 541.

12. Clark, J. A., D. F. Jankowski, H. Merte, Jr., et al., "Pressurization of Liquid Oxygen Containers," Univ. of Mich. Res. Inst. Report 2646-18-P, Ann Arbor, Sept., 1959.

13. Morgan, S. K., and H. F. Brady, "Elimination of the Geysering Effect in Missiles," presented at the Cryogenic Engineering Conference, Aug. 1961, Ann Arbor, Michigan.

14. Data supplied by Geo. C Marshall Space Flight Center, NASA Huntsville, Alabama, C. C. Wood to J. A. Clark (Oct., 1961).

15. "Critical LOX Temperature in Suction Line of H-1 Rocket Engine Prior to Lift-Off," George C. Marshall Space Flight Center, NASA, MTP-M-S and M-P-61-3, Jan. 25, 1961.

16. Smith, S. R., I. Gas-Liquid Phase Equilibria in the System Helium-Hydrogen. II. Development of Mass Spectrometer Techniques for Analysis of Helium-Hydrogen and Their Isotopes. Ph.D. thesis, Ohio State (1952).

17. Forster, H. K., "Diffusion in a Moving Medium with Time-Dependent Boundaries," J. of AIChE, 3, 535 (1957).

18. Carslaw, H. S., and J. C. Jaeger, Conduction of Heat in Solids, 2nd ed., Oxford Press, 1959.

19. Forster, H. K., "On Conduction of Heat into a Growing Vapor Bubble," J. of Appl. Phys., 25, 1067 (1954).

20. Dergarabedian, P., "Rate of Growth of Vapor Bubbles in Superheated Water," J. of Appl. Mech., 20, 537 (1953).

21. Griffith, P., Bubble Growth Rates in Boiling, Tech. Report No. 8, MIT, 1956.

22. Scriven, L. E., "On the Dynamics of Phase Growth," Chem. Eng. Sci., 10, 1-3 (1959).

23. Benjamin, J. E., and J. W. Westwater, "Bubble Growth in Nucleate Boiling of a Binary Mixture," International Development in Heat Transfer, Part II, ASME, 1961, p. 212.

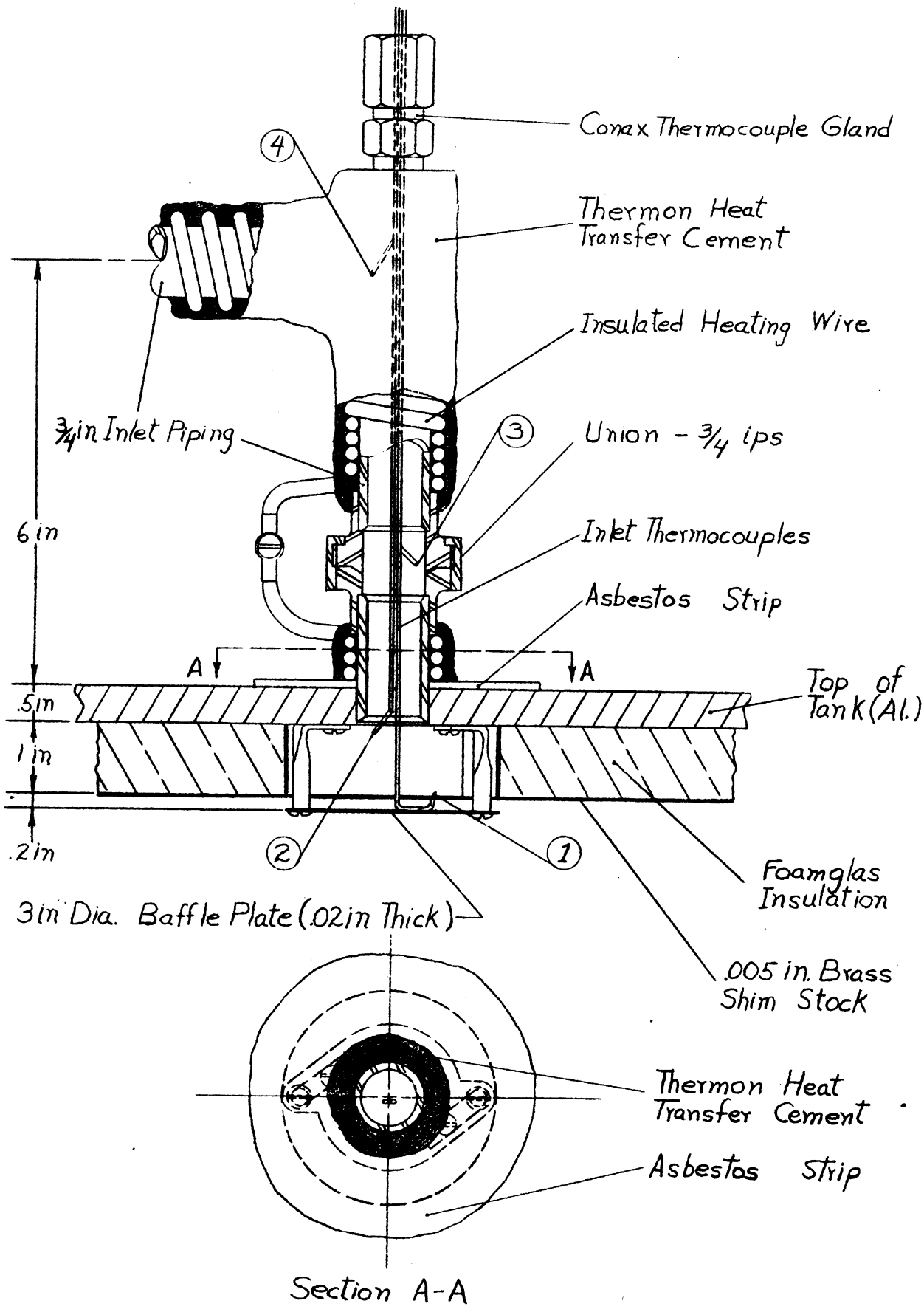


Fig. 1: Inlet Piping Assembly

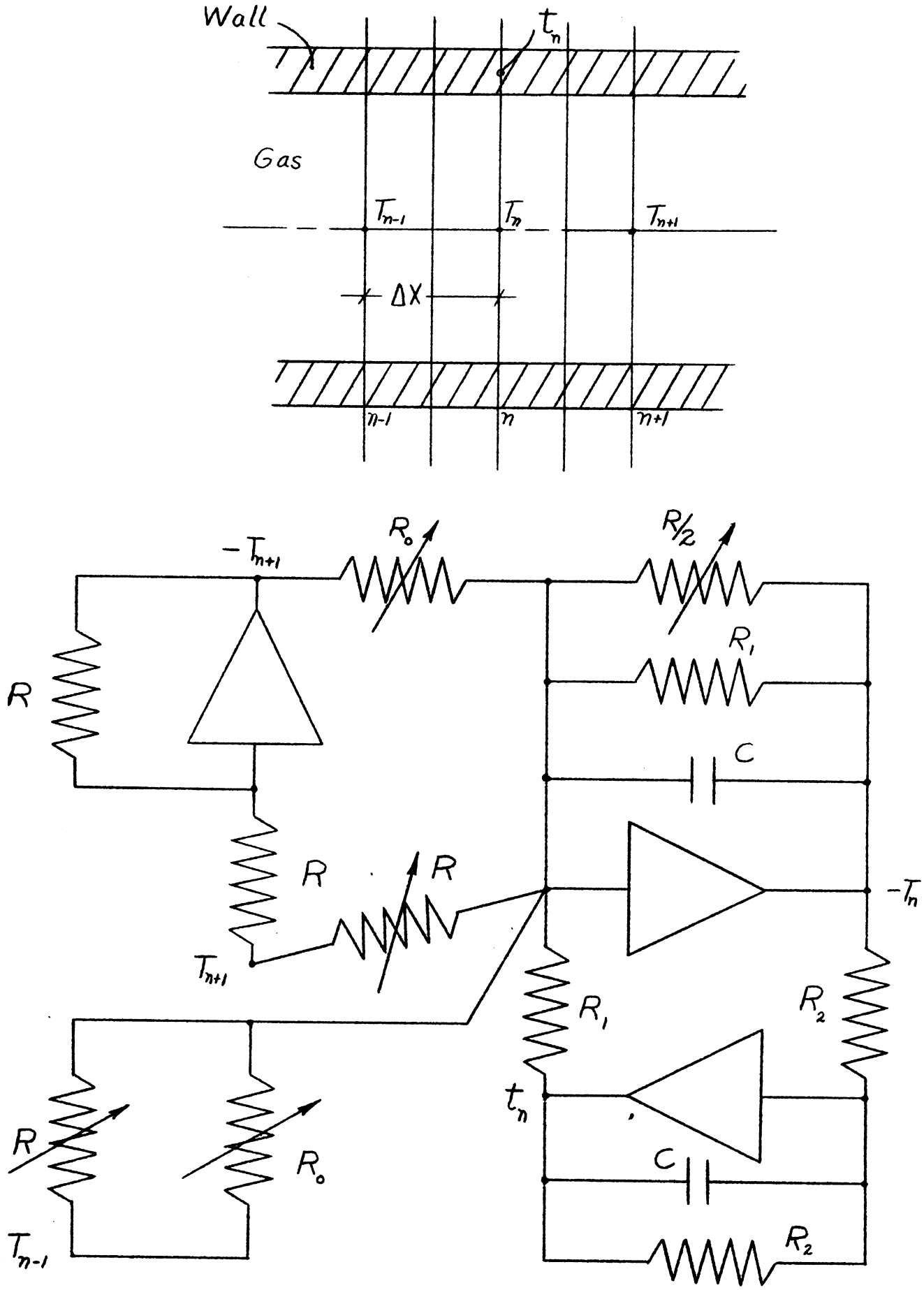


Fig 2: ANALOG COMPUTER CIRCUIT FOR A TYPICAL NODE

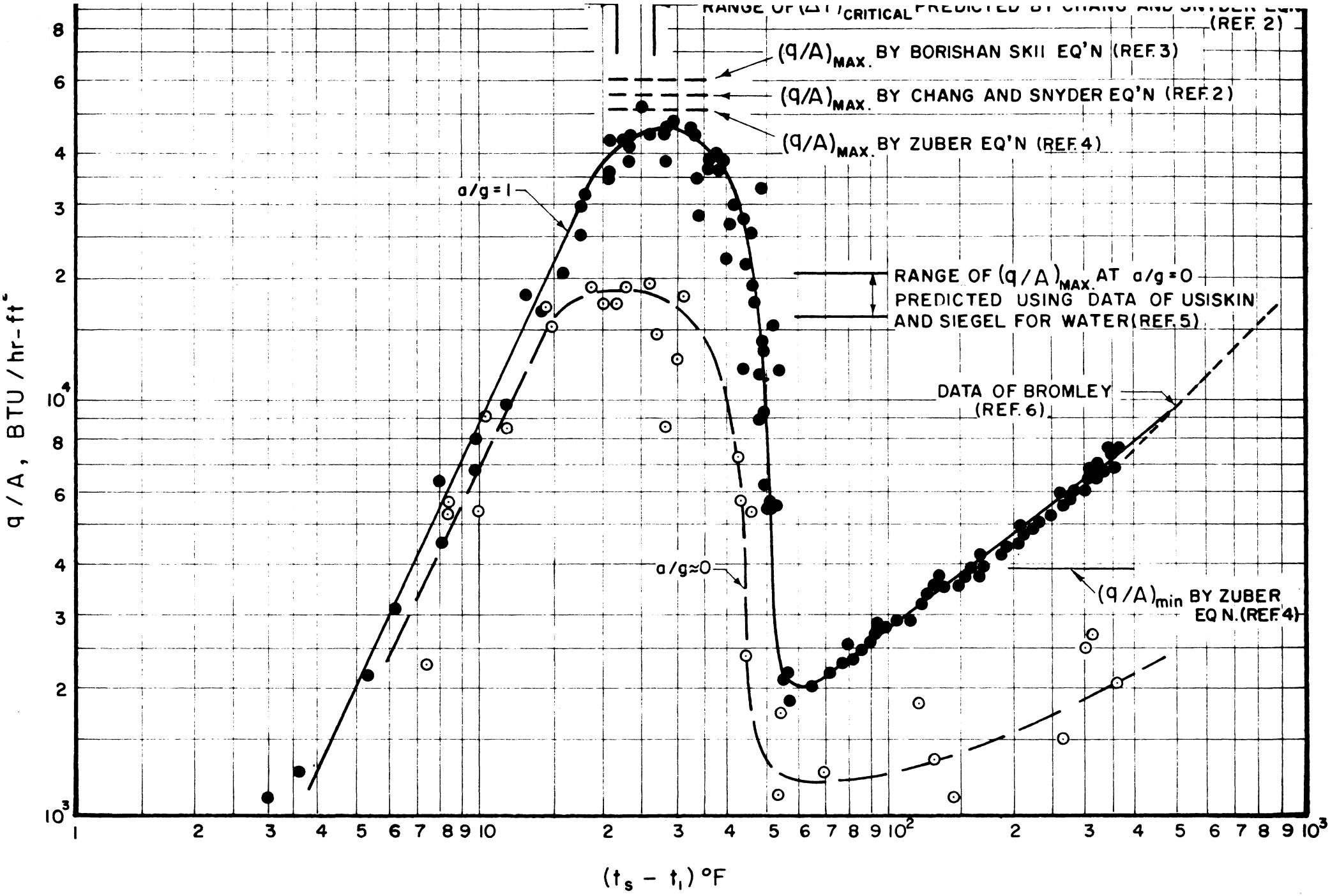


FIGURE 3. BOILING HEAT TRANSFER TO LIQUID NITROGEN AT ATMOSPERIC PRESSURE FROM 1 INCH DIAMETER COPPER SPHERE AT a/g = 1 AND 0

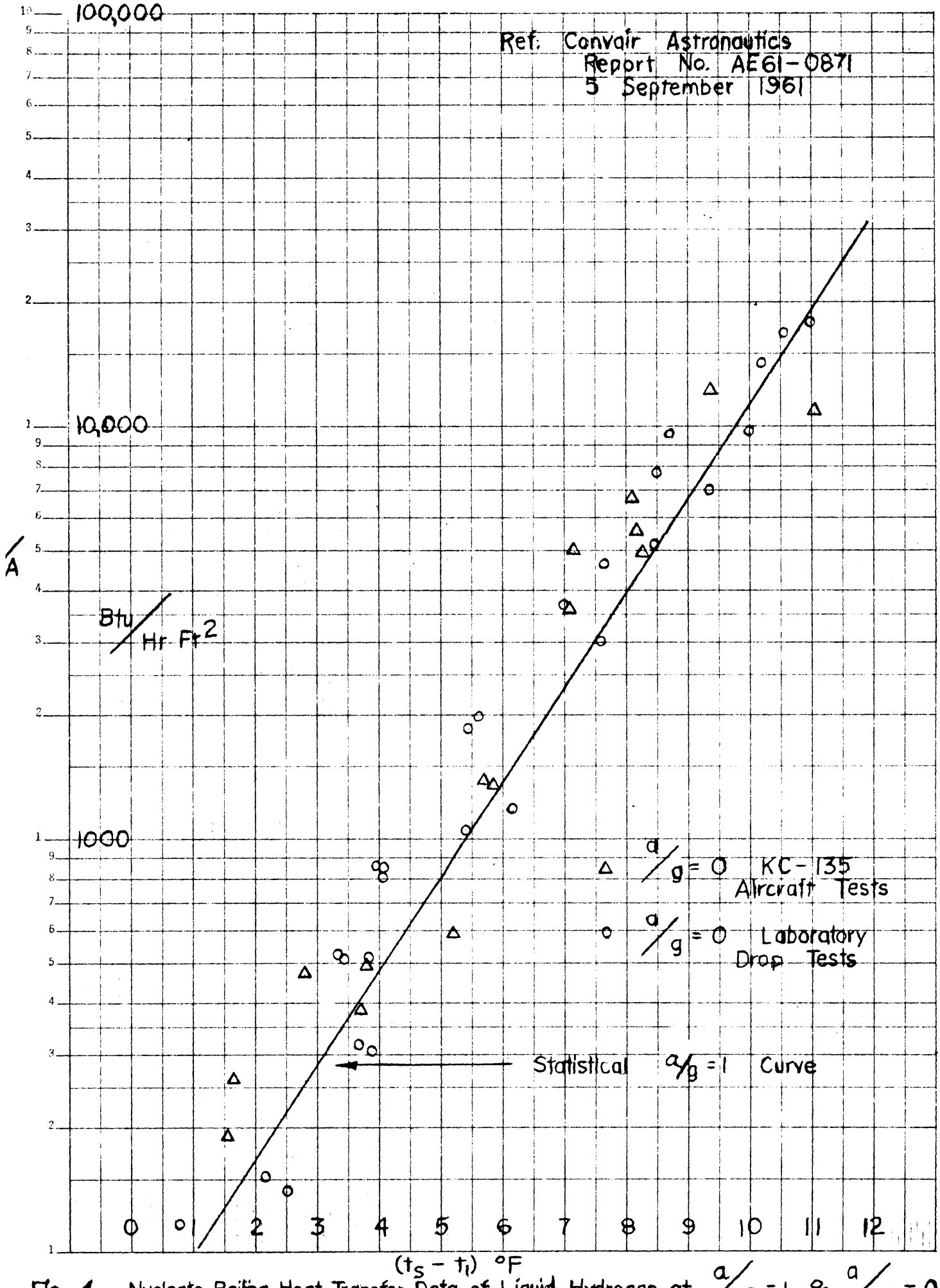


Fig. 4 Nucleate Boiling Heat Transfer Data of Liquid Hydrogen at $a/g = 1$ & $a/g = 0$

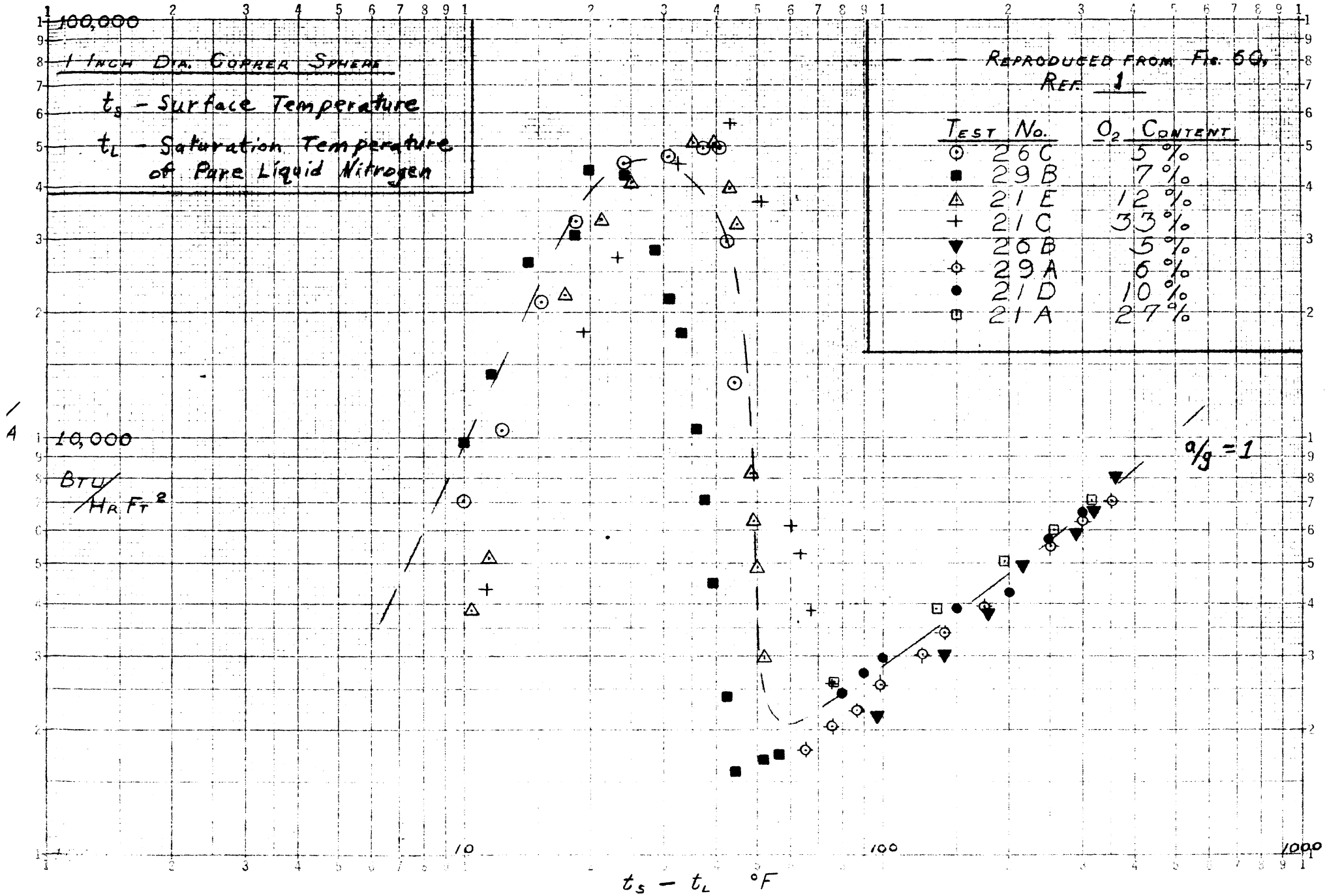


Fig. 5 Boiling Heat Transfer Data of Liquid Nitrogen at a/g = 1 Showing Influence of $O_2$ Impurity

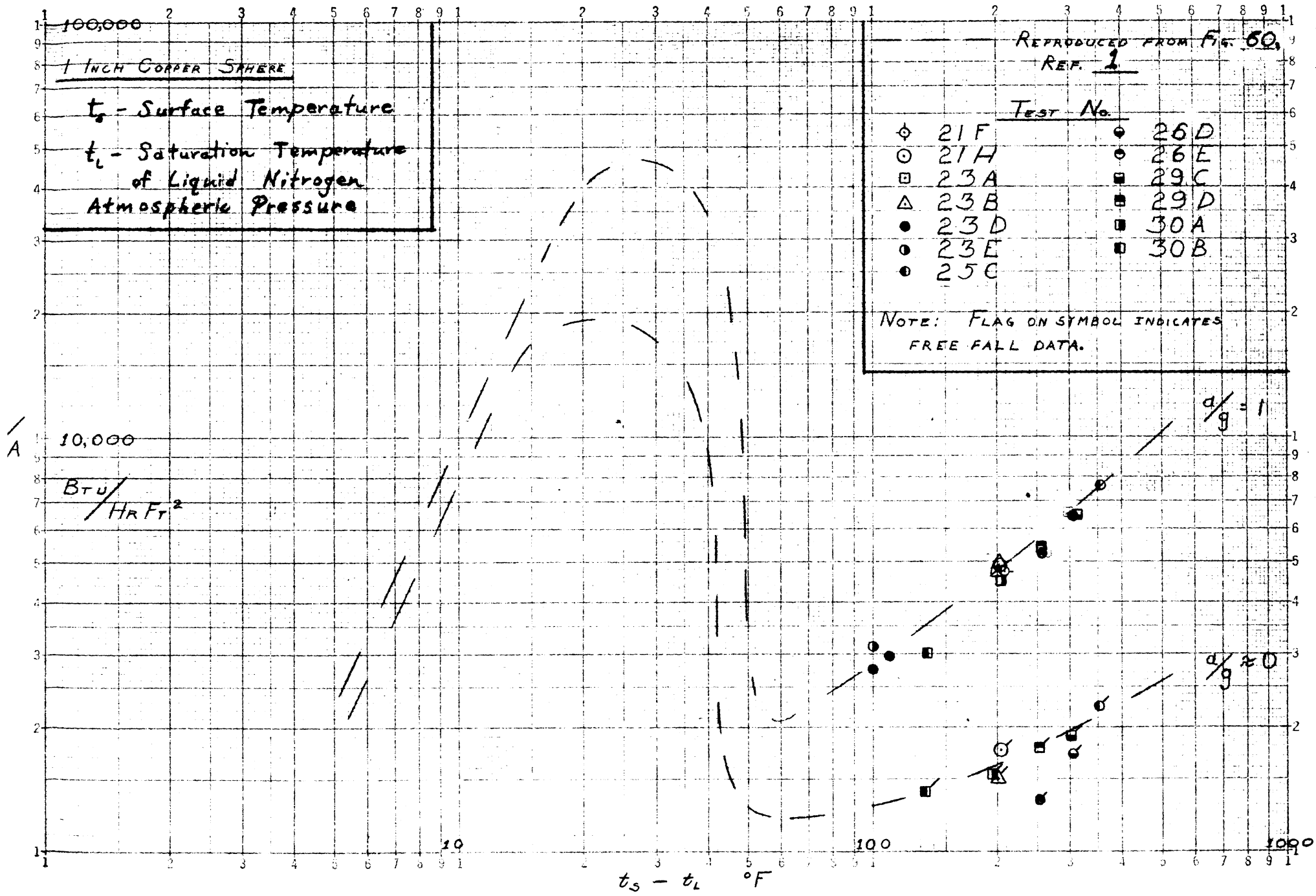


Fig. 6 Film Boiling Heat Transfer Data of Liquid Nitrogen at $a/g \approx 0$

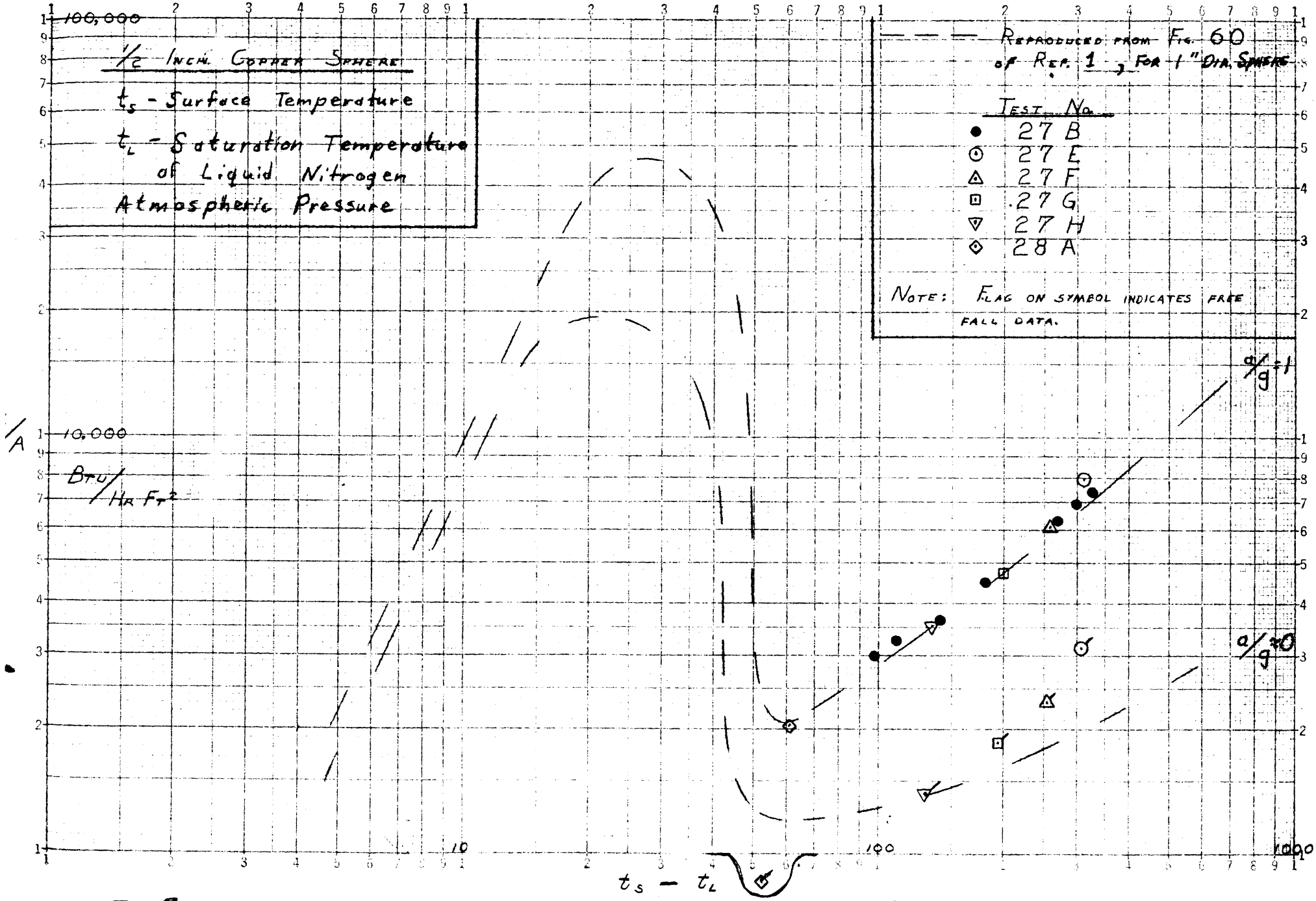


Fig. 7. Film Boiling Heat Transfer Data of Liquid Nitrogen at $a/g = 1$ and $a/g \approx 0$

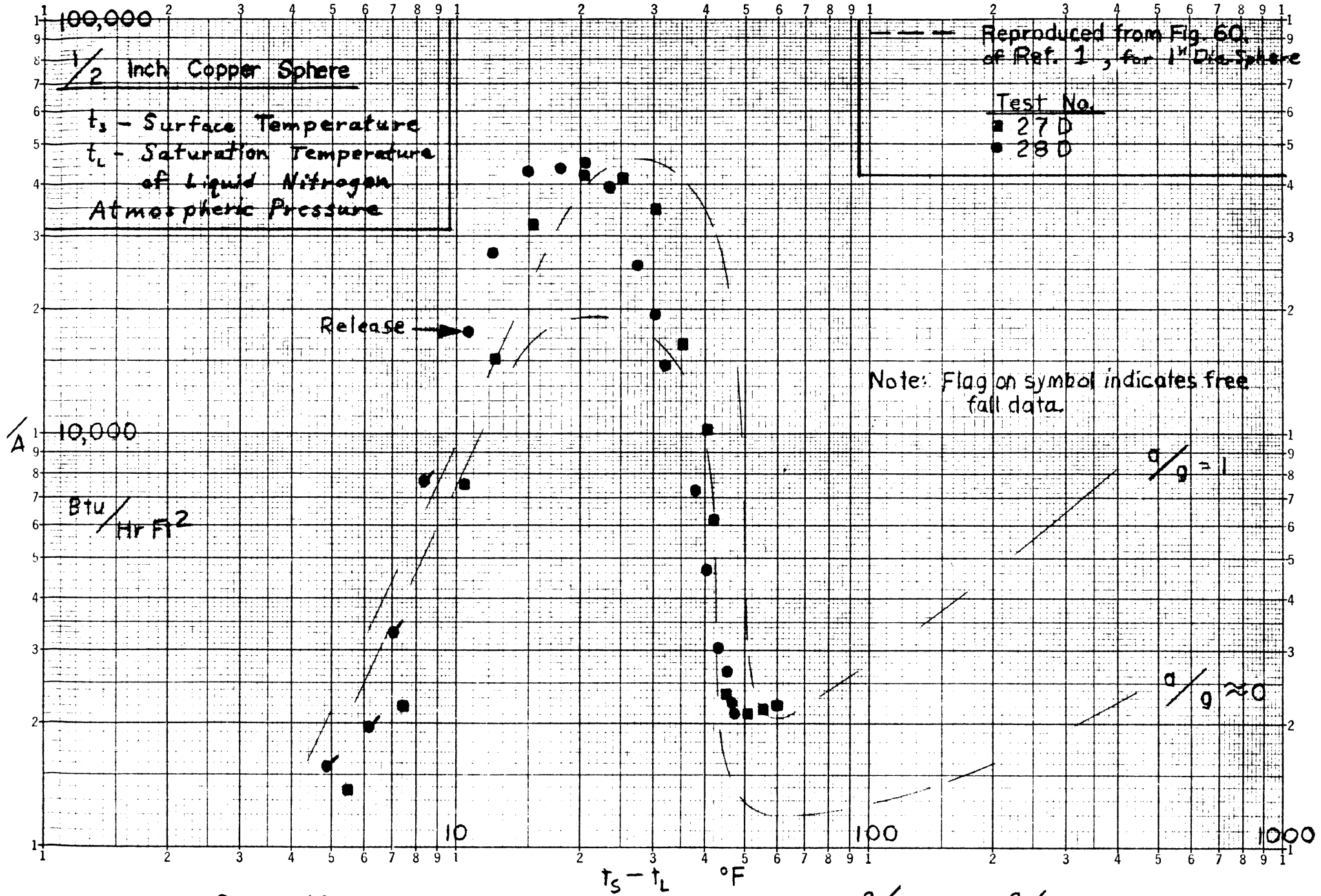


Fig. 8. Boiling Heat Transfer Data of Liquid Nitrogen at $q/g = 1$ & $q/g \approx 0$

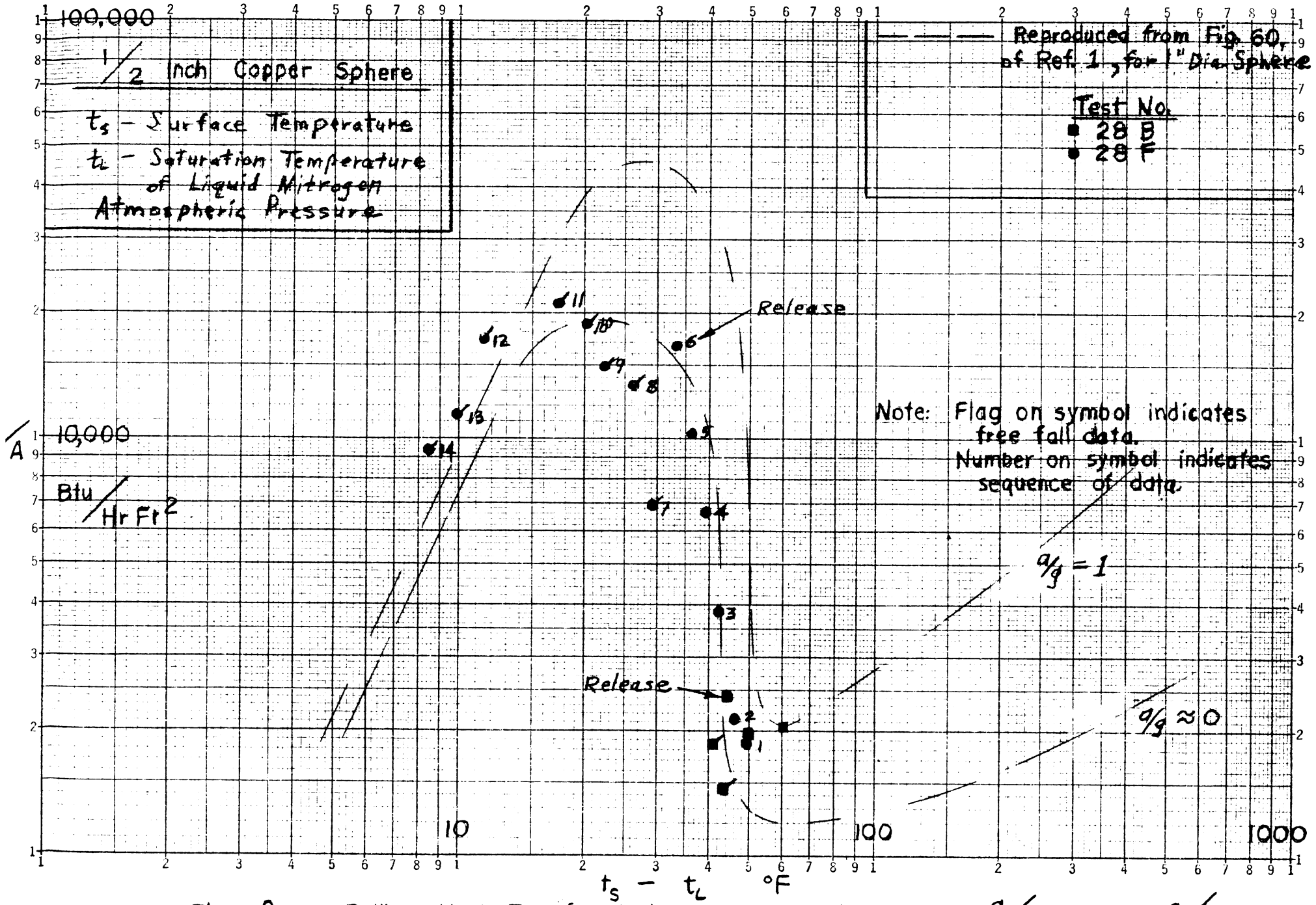


Fig. 9. Boiling Heat Transfer Data of Liquid Nitrogen at $a/g = 1$ & $a/g \approx 0$

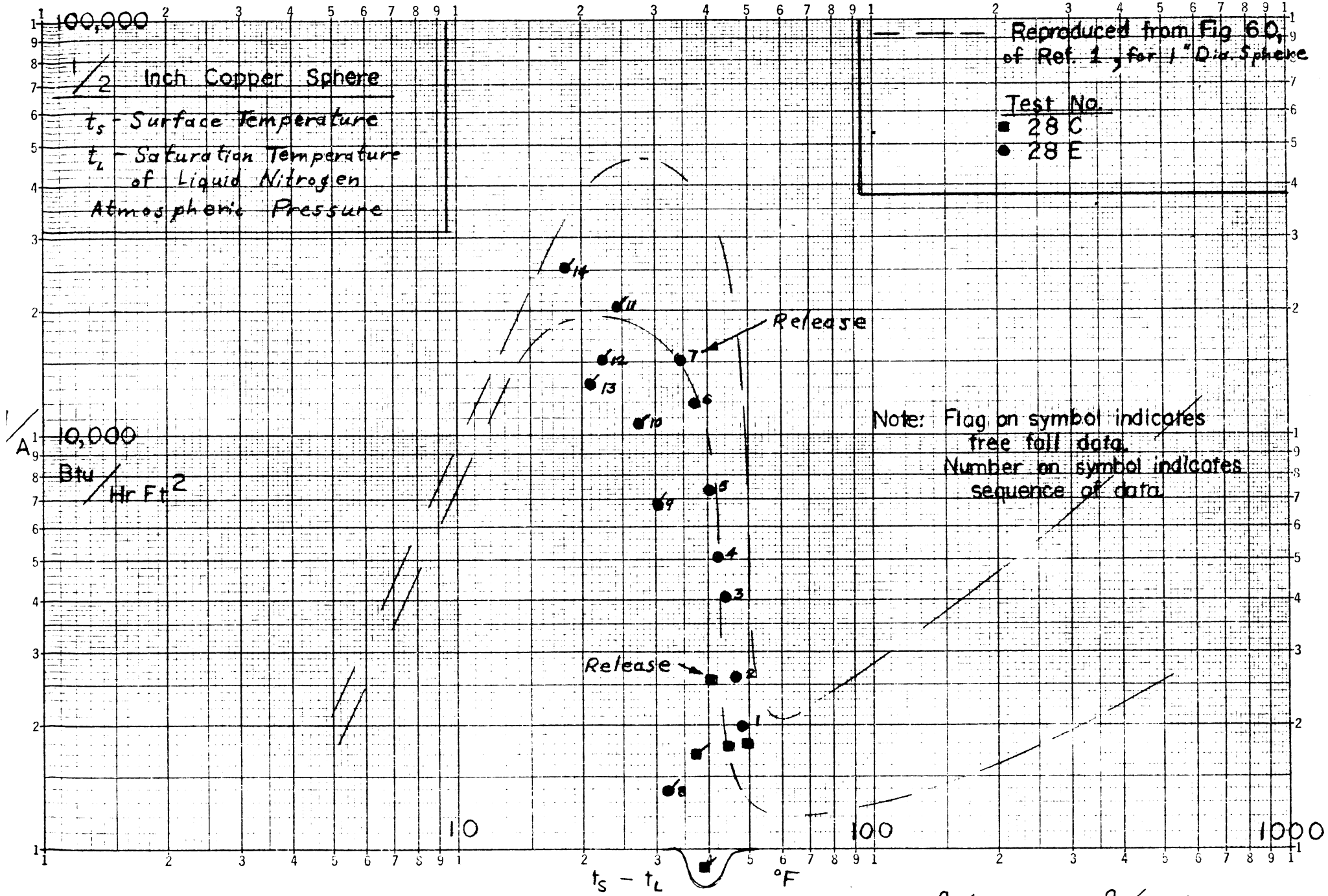


Fig. 10. Boiling Heat Transfer Data of Liquid Nitrogen at $a/g = 1$ & $a/g \approx 0$

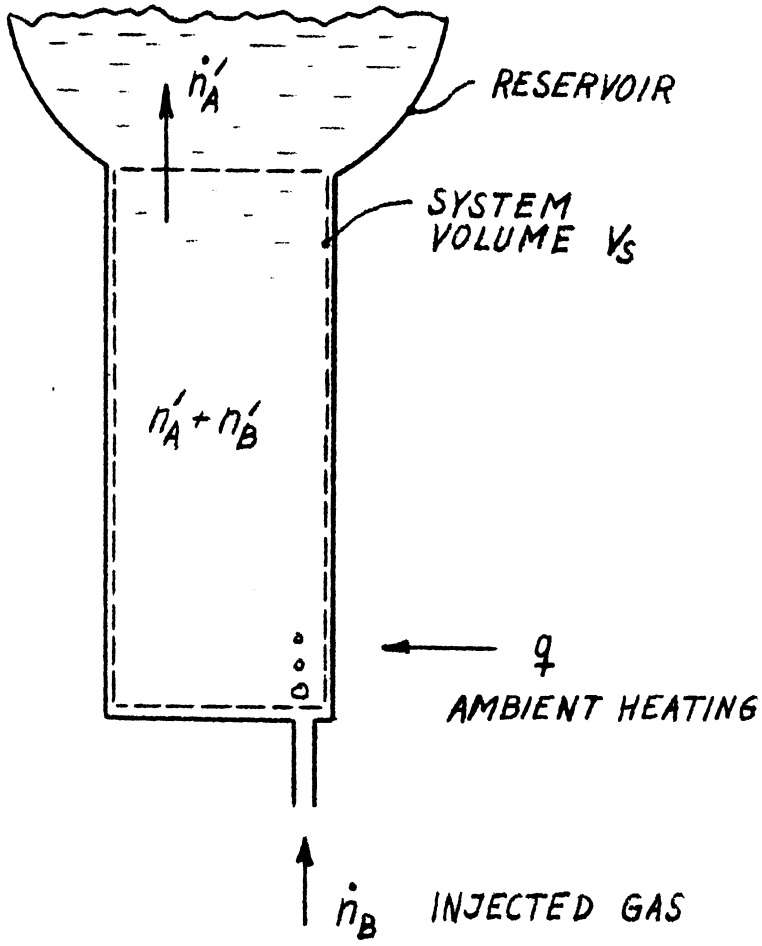


Fig. 11 Analytical Model for Gas Injection with Liquid Phase Present Only.

# TENTATIVE HYDROGEN-HELIUM EQUILIBRIUM

## 120 psia ISOBAR

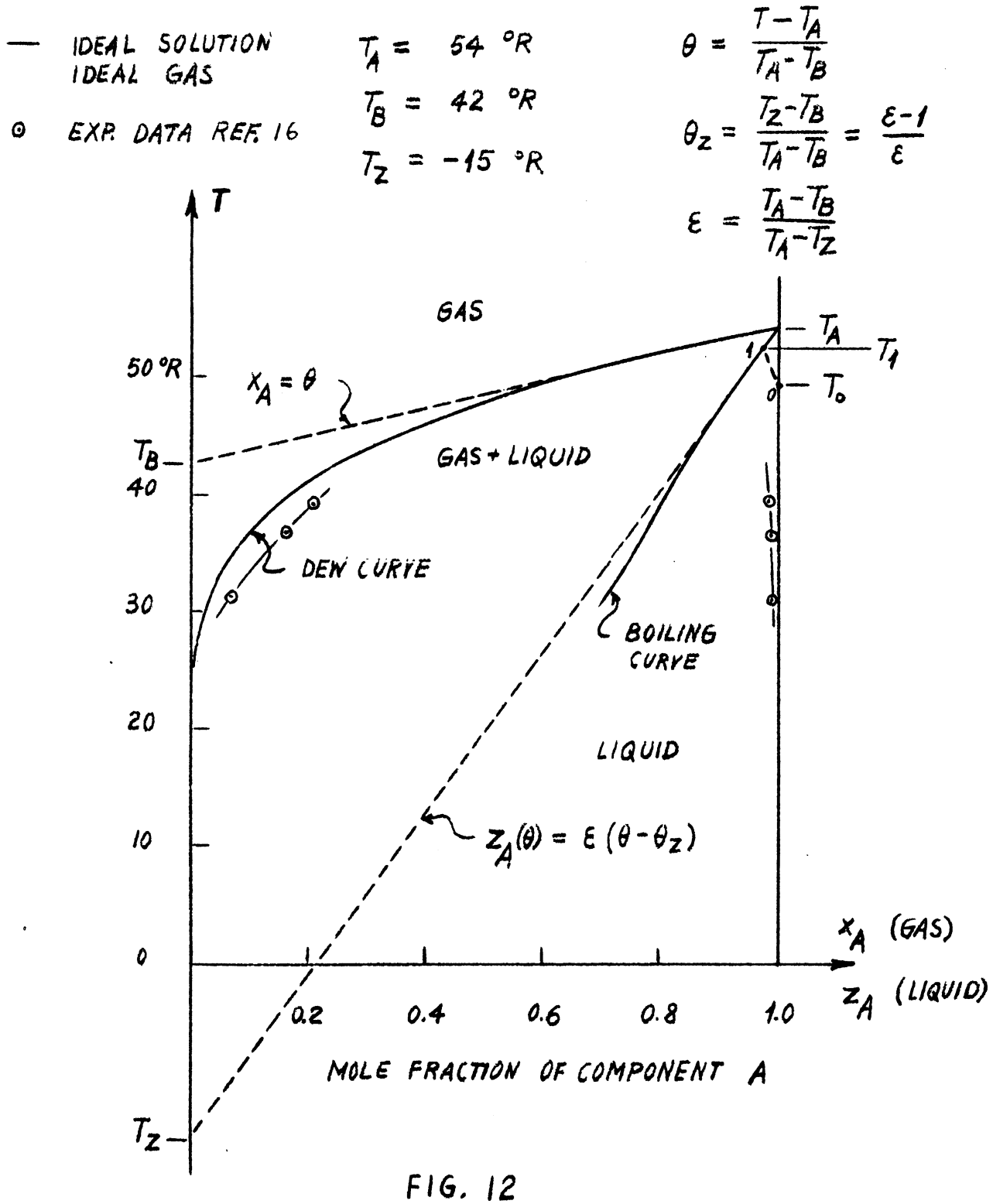


FIG. 12

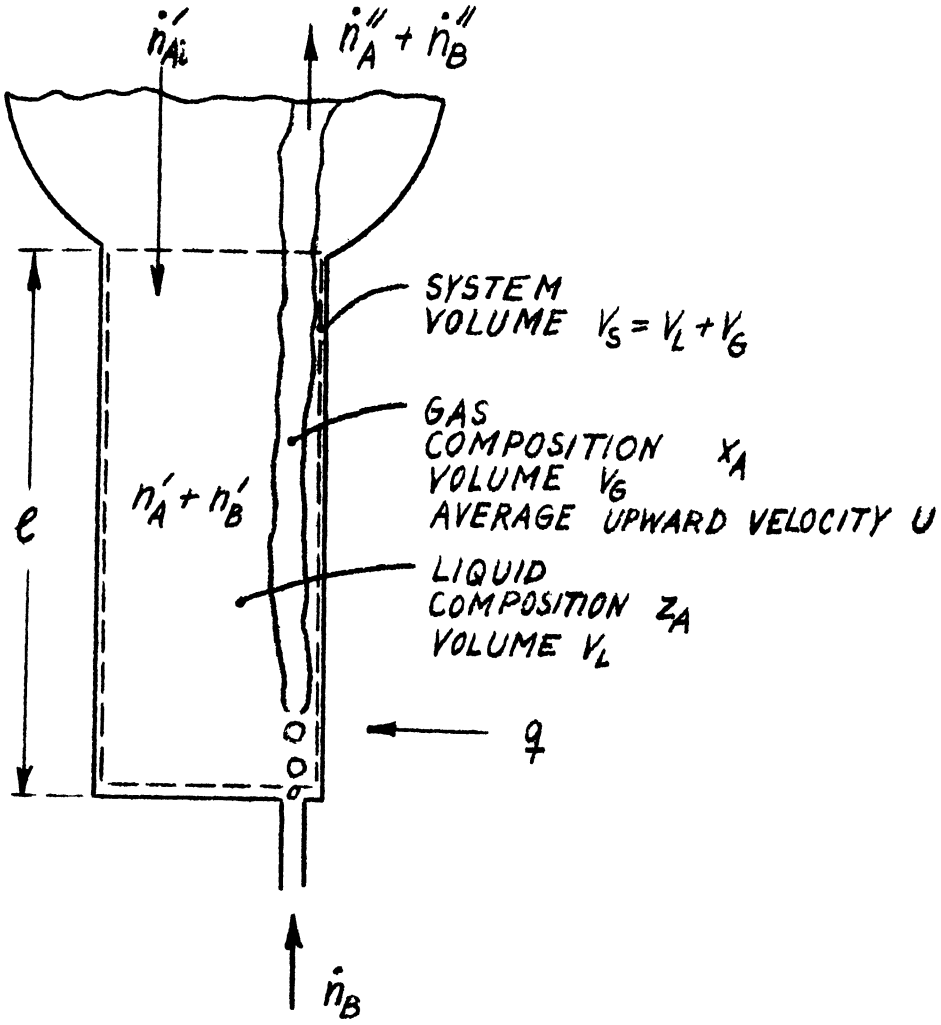


Fig. 13 Analytical Model for Gas Injection with Two-Phase Equilibrium

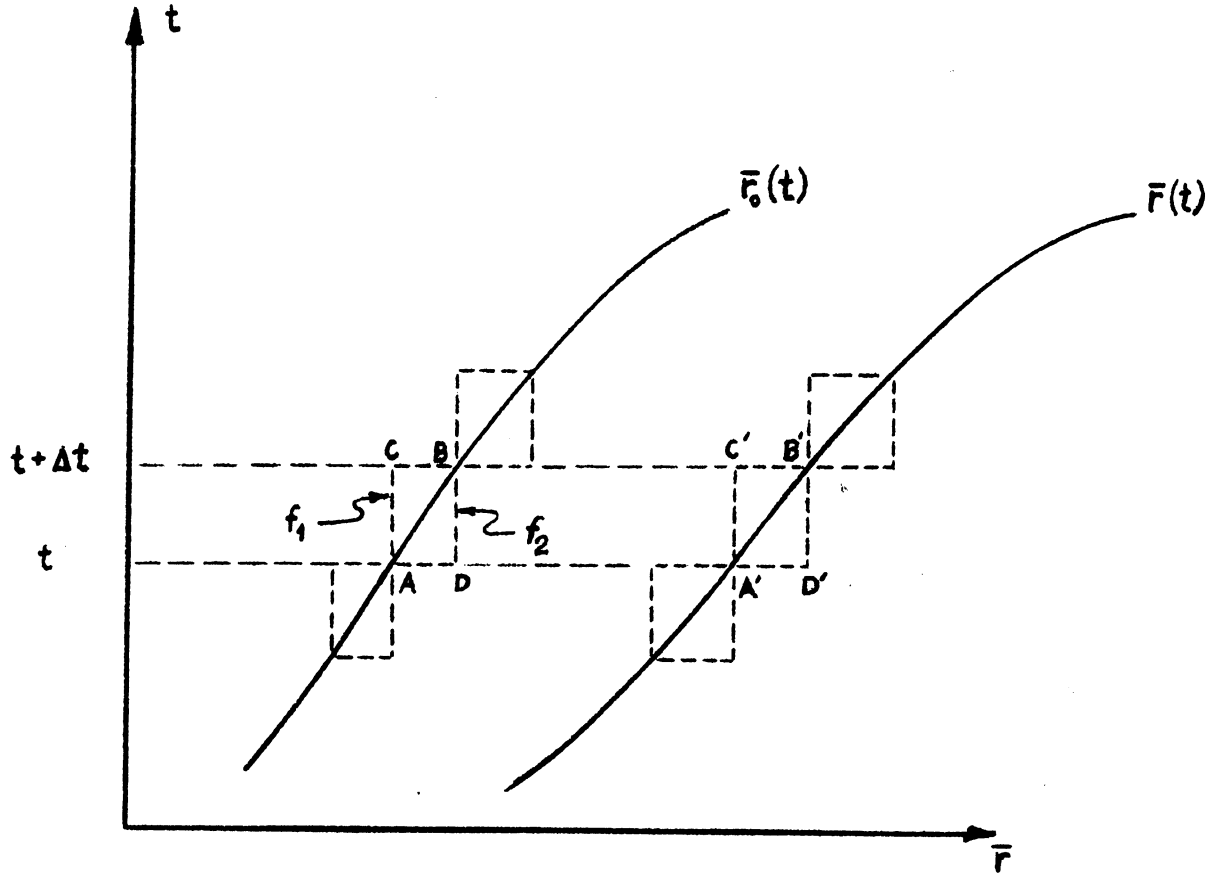


Fig. 14. Space-time domain for heat conduction problem with a moving boundary.